Nuclear medium effects in $\nu_\tau - A$ deep inelastic scattering at DUNE energies

F. Zaidi

Collaborators

Prof. M. Sajjad Athar and Prof. S. K. Singh

Aligarh Muslim University, India

Outline

Introduction

- Among the three generations of the standard model leptons, we know least about the neutral partner (ν_τ) of the third generation weak isospin doublet.

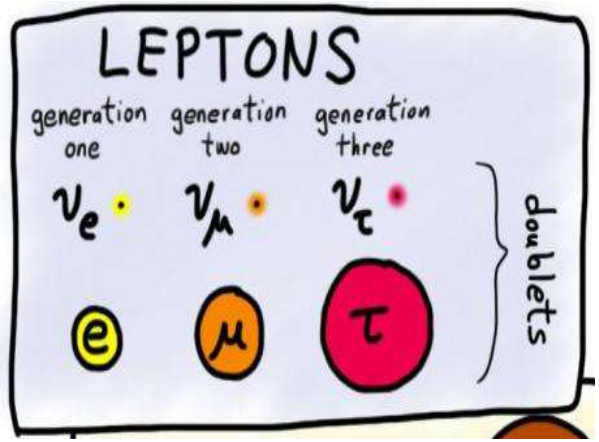

- $\tau-$lepton is ≈ 17 times heavier than muon.
- So, threshold energy for charged current $\nu_\tau - N$ induced τ production is ≈ 3.5 GeV while for μ production it is 110 MeV.
- $\tau-$lepton lifetime is very short ($\approx 10^{-13}$ sec) as compared to muon ($\approx 10^{-6}$ sec).

Introduction

- Among the three generations of the standard model leptons, we know least about the neutral partner (ν_τ) of the third generation weak isospin doublet.

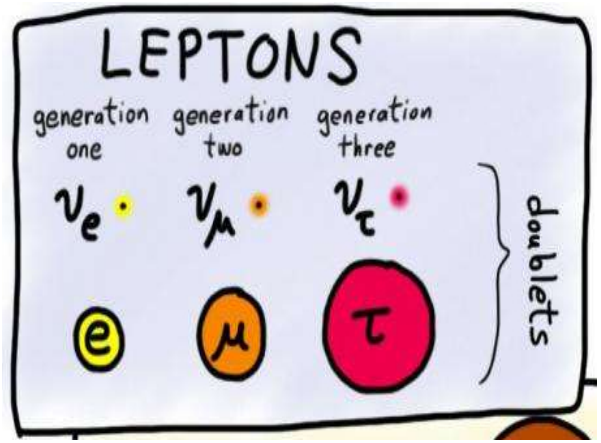

- $\tau-$lepton is ≈ 17 times heavier than muon.
- So, threshold energy for charged current $\nu_\tau - N$ induced τ production is ≈ 3.5 GeV while for μ production it is 110 MeV.
- $\tau-$lepton lifetime is very short ($\approx 10^{-13}$ sec) as compared to muon ($\approx 10^{-6}$ sec).

- DONuT, OPERA, SuperK and IceCube have observed tau (anti)neutrino events but with very limited statistics.
- The cross section of $\nu_\tau - N$ charged current interaction is characterized by considerably larger statistical and systematic uncertainties in comparison to other neutrino flavors.
- Due to limited statistical data, the properties of ν_τ remain insufficiently explored.
- The investigation of $\nu_\tau - N$ cross section holds significance not only for enhancing our understanding of the least explored lepton but also for its practical implications on present and future precision neutrino oscillation experiments.
- The determination of the neutrino interaction cross section holds intrigue as it enables the examination of Lepton Universality.

- The atmospheric neutrino experiments like HyperK, T2HK and IceCube upgrade, plan to observe $\nu_\tau/\bar{\nu}_\tau$ events via $\nu_\mu \to \nu_\tau$ oscillation channel.

- The atmospheric neutrino experiments like HyperK, T2HK and IceCube upgrade, plan to observe $\nu_\tau/\bar{\nu}_\tau$ events via $\nu_\mu \to \nu_\tau$ oscillation channel.
- In the accelerator based experiments such as DUNE, SHiP, FASERν, SND@LHC and DsTau, some are planning to use $\nu_\mu \to \nu_\tau$ oscillation mode as well as from D_s-meson decay mode.

- The atmospheric neutrino experiments like HyperK, T2HK and IceCube upgrade, plan to observe $\nu_\tau/\bar{\nu}_\tau$ events via $\nu_\mu \to \nu_\tau$ oscillation channel.
- In the accelerator based experiments such as DUNE, SHiP, FASERν, SND@LHC and DsTau, some are planning to use $\nu_\mu \to \nu_\tau$ oscillation mode as well as from D_s-meson decay mode.
- Though several theoretical efforts have been made to study $\nu_{e,\mu} - N$ DIS cross sections, but in the case of $\nu_\tau - N$ DIS process only limited studies are available in the literature.

- The atmospheric neutrino experiments like HyperK, T2HK and IceCube upgrade, plan to observe $\nu_\tau/\bar{\nu}_\tau$ events via $\nu_\mu \to \nu_\tau$ oscillation channel.
- In the accelerator based experiments such as DUNE, SHiP, FASERν, SND@LHC and DsTau, some are planning to use $\nu_\mu \to \nu_\tau$ oscillation mode as well as from D_s-meson decay mode.
- Though several theoretical efforts have been made to study $\nu_{e,\mu} - N$ DIS cross sections, but in the case of $\nu_\tau - N$ DIS process only limited studies are available in the literature.

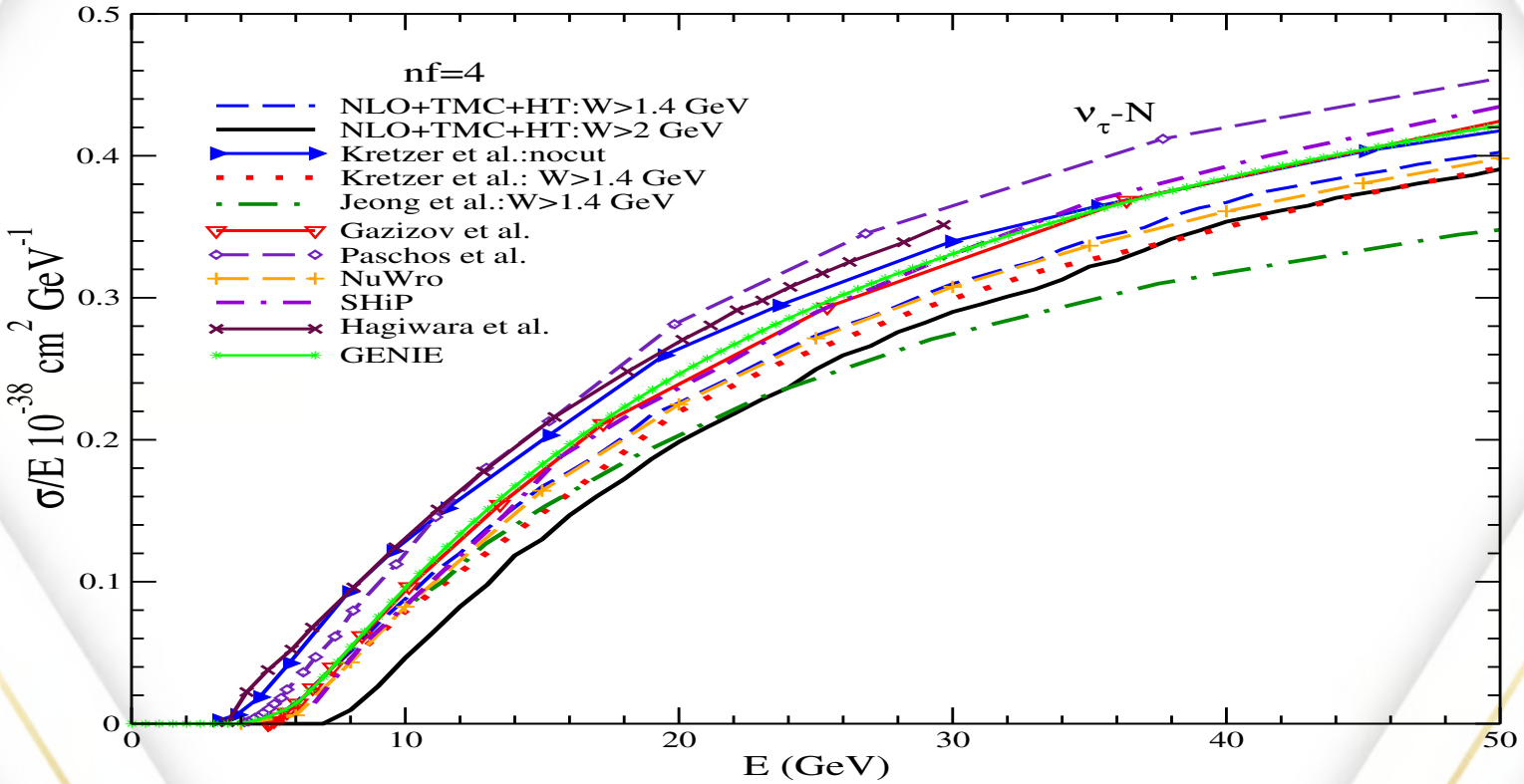

Figure: Cross section for $\nu_\tau - N$ DIS process (**Phys. Rev. D 102 (2020) 11, 113007**).

$\nu - Q^2$ kinematic region

- Because of the absence of any sharp cut on the kinematical variables defining the separation of the SIS and DIS regions, in literature, there is large variation in the consideration of the values of W and Q^2 on the onset of the DIS region.

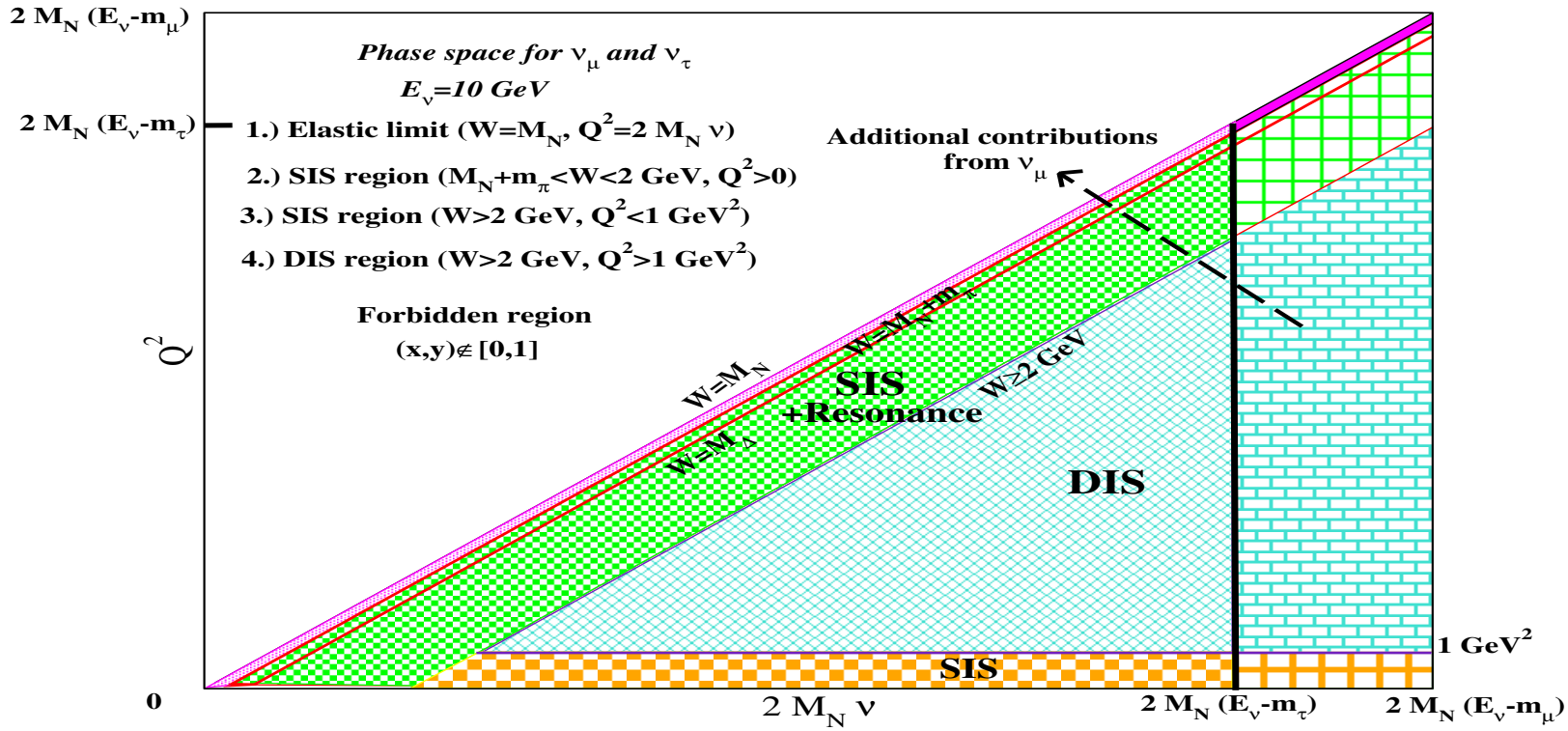

Phys. Rev. D.105 (2022) 3, 033010

- However, nuclear medium effects for $\nu_\tau - A$ DIS process has been studied only by Aligarh group.

$\nu - Q^2$ kinematic region

- Because of the absence of any sharp cut on the kinematical variables defining the separation of the SIS and DIS regions, in literature, there is large variation in the consideration of the values of W and Q^2 on the onset of the DIS region.

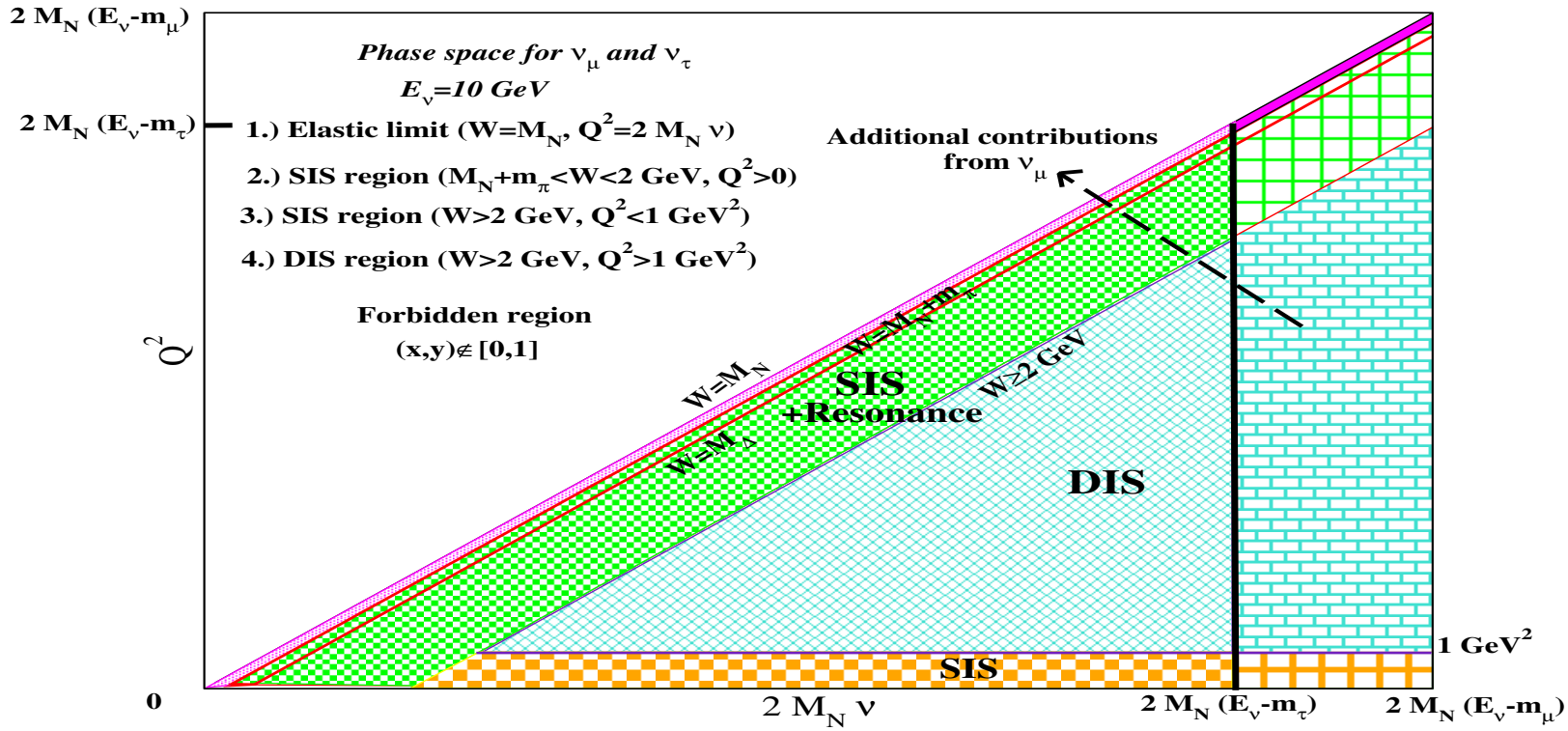

Phys. Rev. D.105 (2022) 3, 033010

- However, nuclear medium effects for $\nu_\tau - A$ DIS process has been studied only by Aligarh group.
- More experimental as well as theoretical efforts are required for the better determination of scattering cross section.

$\nu_\tau - N$ DIS

The differential scattering cross section for $\nu_\tau - N$ DIS process is given by:

$$\nu_\tau/\bar{\nu}_\tau(k) + N(p) \to \tau^-/\tau^+(k') + X(p')$$

$$\frac{d^2\sigma_N}{dxdy} = \frac{G_F^2 y}{16\pi}\left(\frac{M_W^2}{Q^2+M_W^2}\right)^2 L^{\alpha\beta} W^N_{\alpha\beta},$$

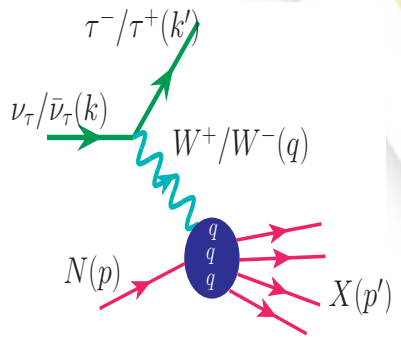

where the leptonic tensor is written as

$$L^{\alpha\beta} = k^\alpha k'^\beta + k'^\alpha k^\beta - k\cdot k' g^{\alpha\beta} \pm i\varepsilon^{\alpha\beta\rho\sigma} k_\rho k'_\sigma,$$

and the nucleon hadronic tensor is given by

$$W^N_{\alpha\beta} = -g_{\alpha\beta} W_{1N}(x,Q^2) + p_\alpha p_\beta \frac{W_{2N}(x,Q^2)}{M_N^2} - \frac{i}{M_N^2}\varepsilon_{\alpha\beta\rho\sigma} p^\rho q^\sigma W_{3N}(x,Q^2)$$
$$+ \frac{q_\alpha q_\beta}{M_N^2} W_{4N}(x,Q^2) + (p_\alpha q_\beta + p_\beta q_\alpha)\frac{W_{5N}(x,Q^2)}{M_N^2}.$$

$W_{iN}(x,Q^2)$ are related to the dimensionless nucleon structure functions $F_{iN}(x,Q^2)$:

$$F_{1N}(x) = W_{1N}(\nu,Q^2);\quad F_{2N}(x) = \frac{Q^2}{2xM_N^2} W_{2N}(\nu,Q^2);\quad F_{3N}(x) = \frac{Q^2}{xM_N^2} W_{3N}(\nu,Q^2)$$

$$F_{4N}(x) = \frac{Q^2}{2M_N^2} W_{4N};\quad F_{5N}(x) = \frac{Q^2}{2xM_N^2} W_{5N}.$$

The differential scattering cross section for the case of massive lepton is:

$$\frac{d^2\sigma_N}{dxdy} = \frac{G_F^2 M_N E_\nu}{\pi(1+\frac{Q^2}{M_W^2})^2}\left\{\left(y^2 x + \frac{m_l^2 y}{2E_\nu M_N}\right)F_{1N}(x,Q^2) + \left[\left(1-\frac{m_l^2}{4E_\nu^2}\right) - \left(1+\frac{M_N x}{2E_\nu}\right)y\right]F_{2N}(x,Q^2)\right.$$
$$\left. \pm \left[xy\left(1-\frac{y}{2}\right) - \frac{m_l^2 y}{4E_\nu M_N}\right]F_{3N}(x,Q^2) + \frac{m_l^2(m_l^2+Q^2)}{4E_\nu^2 M_N^2 x}F_{4N}(x,Q^2) - \frac{m_l^2}{E_\nu M_N}F_{5N}(x,Q^2)\right\},$$

The differential scattering cross section for the case of massive lepton is:

$$\frac{d^2\sigma_N}{dxdy} = \frac{G_F^2 M_N E_\nu}{\pi(1+\frac{Q^2}{M_W^2})^2}\left\{\left(y^2 x + \frac{m_l^2 y}{2E_\nu M_N}\right)F_{1N}(x,Q^2) + \left[\left(1-\frac{m_l^2}{4E_\nu^2}\right) - \left(1+\frac{M_N x}{2E_\nu}\right)y\right]F_{2N}(x,Q^2)\right.$$
$$\left. \pm \left[xy\left(1-\frac{y}{2}\right) - \frac{m_l^2 y}{4E_\nu M_N}\right]F_{3N}(x,Q^2) + \frac{m_l^2(m_l^2+Q^2)}{4E_\nu^2 M_N^2 x}F_{4N}(x,Q^2) - \frac{m_l^2}{E_\nu M_N}F_{5N}(x,Q^2)\right\},$$

x and y are scaling variables and given by:

$$\frac{m_l^2}{2M_N(E_\nu - m_l)} < x < 1$$
$$(a-b) < y < (a+b),$$

with

$$a = \frac{1 - m_l^2\left(\frac{1}{2M_N E_\nu x} + \frac{1}{2E_\nu^2}\right)}{2\left(1+\frac{M_N x}{2E_\nu}\right)}$$

$$b = = \frac{\sqrt{\left(1-\frac{m_l^2}{2M_N E_\nu x}\right)^2 - \frac{m_l^2}{E_\nu^2}}}{2\left(1+\frac{M_N x}{2E_\nu}\right)}.$$

The differential scattering cross section for the case of massive lepton is:

$$\frac{d^2\sigma_N}{dxdy} = \frac{G_F^2 M_N E_\nu}{\pi(1+\frac{Q^2}{M_W^2})^2}\left\{\left(y^2 x+\frac{m_l^2 y}{2E_\nu M_N}\right)F_{1N}(x,Q^2)+\left[\left(1-\frac{m_l^2}{4E_\nu^2}\right)-\left(1+\frac{M_N x}{2E_\nu}\right)y\right]F_{2N}(x,Q^2)\right.$$
$$\left.\pm\left[xy\left(1-\frac{y}{2}\right)-\frac{m_l^2 y}{4E_\nu M_N}\right]F_{3N}(x,Q^2)+\frac{m_l^2(m_l^2+Q^2)}{4E_\nu^2 M_N^2 x}F_{4N}(x,Q^2)-\frac{m_l^2}{E_\nu M_N}F_{5N}(x,Q^2)\right\},$$

x and y are scaling variables and given by:

$$\frac{m_l^2}{2M_N(E_\nu - m_l)} < x < 1$$
$$(a-b) < y < (a+b),$$

with

$$a = \frac{1-m_l^2\left(\frac{1}{2M_N E_\nu x}+\frac{1}{2E_\nu^2}\right)}{2\left(1+\frac{M_N x}{2E_\nu}\right)}$$

$$b = = \frac{\sqrt{\left(1-\frac{m_l^2}{2M_N E_\nu x}\right)^2-\frac{m_l^2}{E_\nu^2}}}{2\left(1+\frac{M_N x}{2E_\nu}\right)}.$$

Nucleon structure functions are generally written in terms of parton distribution functions,e.g. at LO:

$$F_{2N}(x) = \sum_i x[q_i(x)+\bar{q}_i(x)];$$
$$xF_{3N}(x) = \sum_i x[q_i(x)-\bar{q}_i(x)];$$

Callan-Gross relation:

$$2xF_{1N}(x) = F_{2N}(x).$$

Albright-Jarlskog relations:

$$F_{4N}(x) = 0.$$
$$2xF_{5N}(x) = F_{2N}(x).$$

Above relations are true at leading order only.

Next-to-Leading Order(NLO)

- In the naive parton model,

$$F_{1N}(x,Q^2) \xrightarrow[Q^2\to\infty,\nu\to\infty]{x\to finite} F_{1N}(x)$$

$$F_{2N}(x,Q^2) \xrightarrow[Q^2\to\infty,\nu\to\infty]{x\to finite} F_{2N}(x)$$

- The QCD improved naive parton model allows quarks to interact among themselves via the gluon exchange.

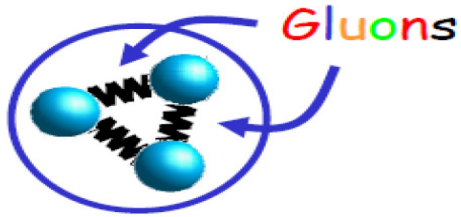

- Gluon emission introduces the Q^2 dependence in structure functions.
- The nucleon structure functions in terms of the convolution of coefficient function (H_f ; $(f = q, g)$) with the density distribution of partons (f) inside the nucleon is:

$$x^{-1}F_i(x) = \sum_{f=q,g} H_f^{(n)}(x) \otimes f(x)\ , i = 1-5$$

$$H_f(x) \otimes f(x) = \int_x^1 H_f(y)\, f\left(\frac{x}{y}\right)\frac{dy}{y}$$

Target Mass Correction

- At finite Q^2 heavy quarks are produced like strange, charm, etc.
- Heavy quarks production modifiy the scattering kinematics, therefore, for massless quarks

$$x \to \xi$$

$$\xi = \frac{2x}{1+\sqrt{1+4\mu x^2}}, \qquad \mu = \frac{M_N^2}{Q^2}$$

- For the massive partons, the Nachtmann variable ξ gets modified to the slow rescaling variable $\bar{\xi}$:

$$\bar{\xi} = \xi\left(1+\frac{m_c^2}{Q^2}\right) = \frac{\xi}{\lambda}$$

$$\lambda = \frac{Q^2}{(Q^2+m_c^2)}$$

- This effect is known as target mass correction (TMC)
- TMC is effective at low Q^2 and high x, where PDFs are not very well determined.

Higher Twist Correction

- Twist-4 ($\tau = 4$) term, reflects the strength of multi-parton correlations.
- The unpolarized structure functions can be expressed in the powers of $1/Q^2$ as:

$$F_i(x,Q^2) = F_i^{\tau=2}(x,Q^2)\left(1 + \frac{H_i^{\tau=4}(x)}{Q^2}\right) \quad i = 1,2,3,$$

$\tau = 2$ is the twist-2 or leading twist term and $\tau = 4$ corresponds to twist-4 or higher twist term.

- HT is inorporated following the works of Dasgupta et al. (Phys. Lett. B **382**, 273 (1996).)

$$H_i^{\tau=4}(x,Q^2) = A_2' \int_x^1 \frac{dz}{z}\, C_2^i(z)\, q\left(\frac{x}{z}, Q^2\right),$$

with $i = 1,2,3$. C_2^i is the coefficient function for twist-4, A_2' is the constant parameter and $q(x/z, Q^2)$ is the quarks density distribution.

QCD Corrections

- Present calculations have been performed by taking into account various perturbative and nonperturbative effects such as target mass correction (TMC), higher twist (HT) and evolution of parton densities at next-to-leading order (NLO) along with the effect of tau lepton mass, charm quark mass, etc.
- We have considered four flavor scheme by treating up, down and strange quarks to be massless while charm quark as a massive object. Therefore, the nucleon structure functions are written as:

$$F_{n_f=4}(x,Q^2) = \underbrace{F_{n_f=3}(x,Q^2)}_{\textit{massless quarks}} + \underbrace{F_{n_f=1}(x,Q^2)}_{\textit{massive charm}}$$

- Charm quark mass is taken to be 1.3 GeV.
- The threshold for the τ^- production in $\nu_\tau N \to \tau^- N$ is about 3.45 GeV.
- We have followed the works of Kretzer et al. and Jeong et al.

Phys. Rev. D **66**, 113007 (2002),
Phys. Rev. D **69**, 034002 (2004),
Phys. Rev. D **82**, 033010 (2010).

Free nucleon structure functions

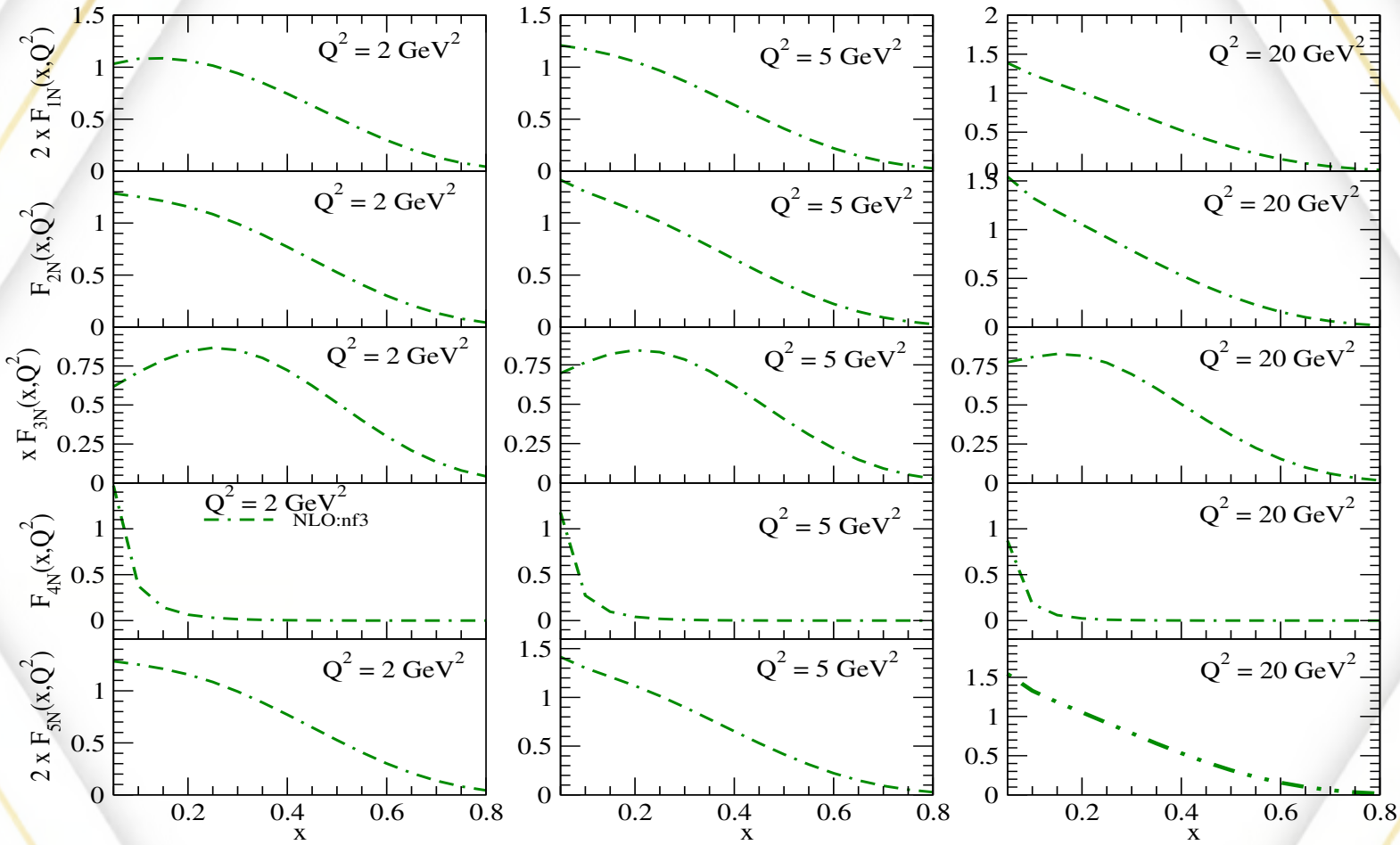

Figure: Results for free nucleon structure functions $F_{iN}(x,Q^2);(i=1-5)$ at different values of Q^2 are shown.

Phys. Rev. D.102 (2020) 11, 113007

Free nucleon structure functions

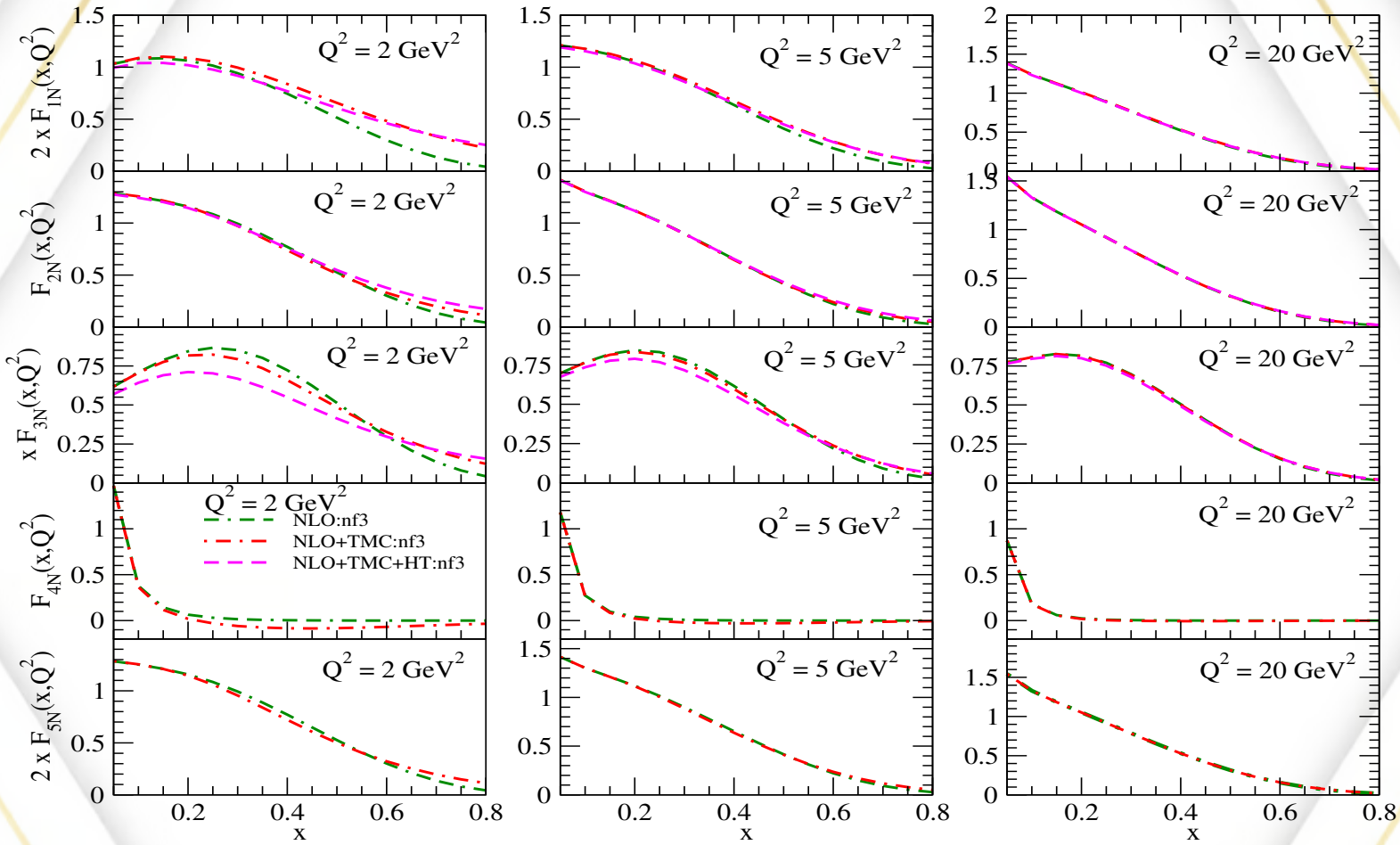

Figure: Results for free nucleon structure functions $F_{iN}(x,Q^2);(i=1-5)$ at different values of Q^2 are shown.

Phys. Rev. D.102 (2020) 11, 113007

Free nucleon structure functions

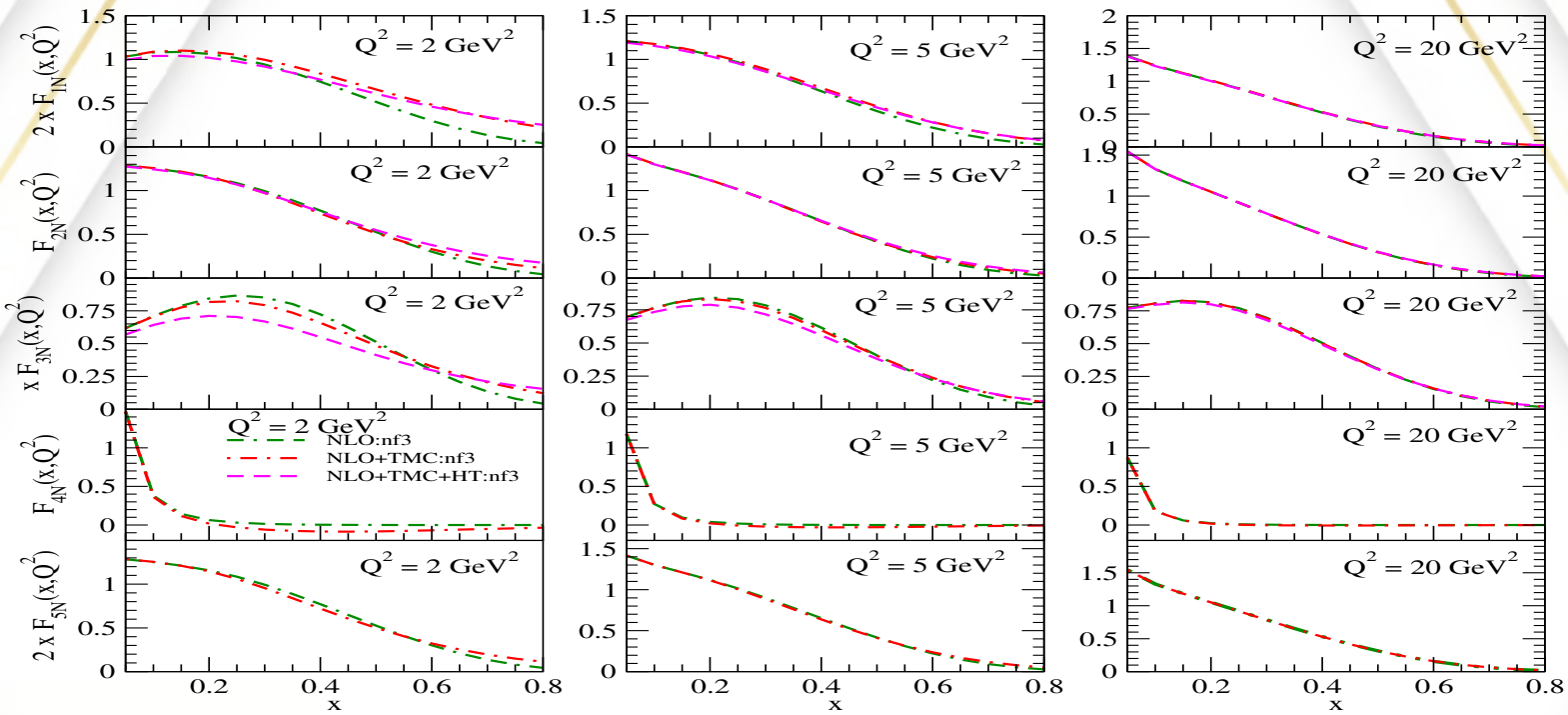

$Q^2(GeV^2)$	x	$(HT-TMC)*100/TMC$		
		$F_{1N}(x,Q^2)$	$F_{2N}(x,Q^2)$	$F_{3N}(x,Q^2)$
2	0.3	2%	$< 1\%$	20%
	0.8	27%	35%	$\approx 21\%$

Figure: Results for free nucleon structure functions $F_{iN}(x,Q^2);(i=1-5)$ at different values of Q^2 are shown.

Phys. Rev. D.102 (2020) 11, 113007

Free nucleon structure functions

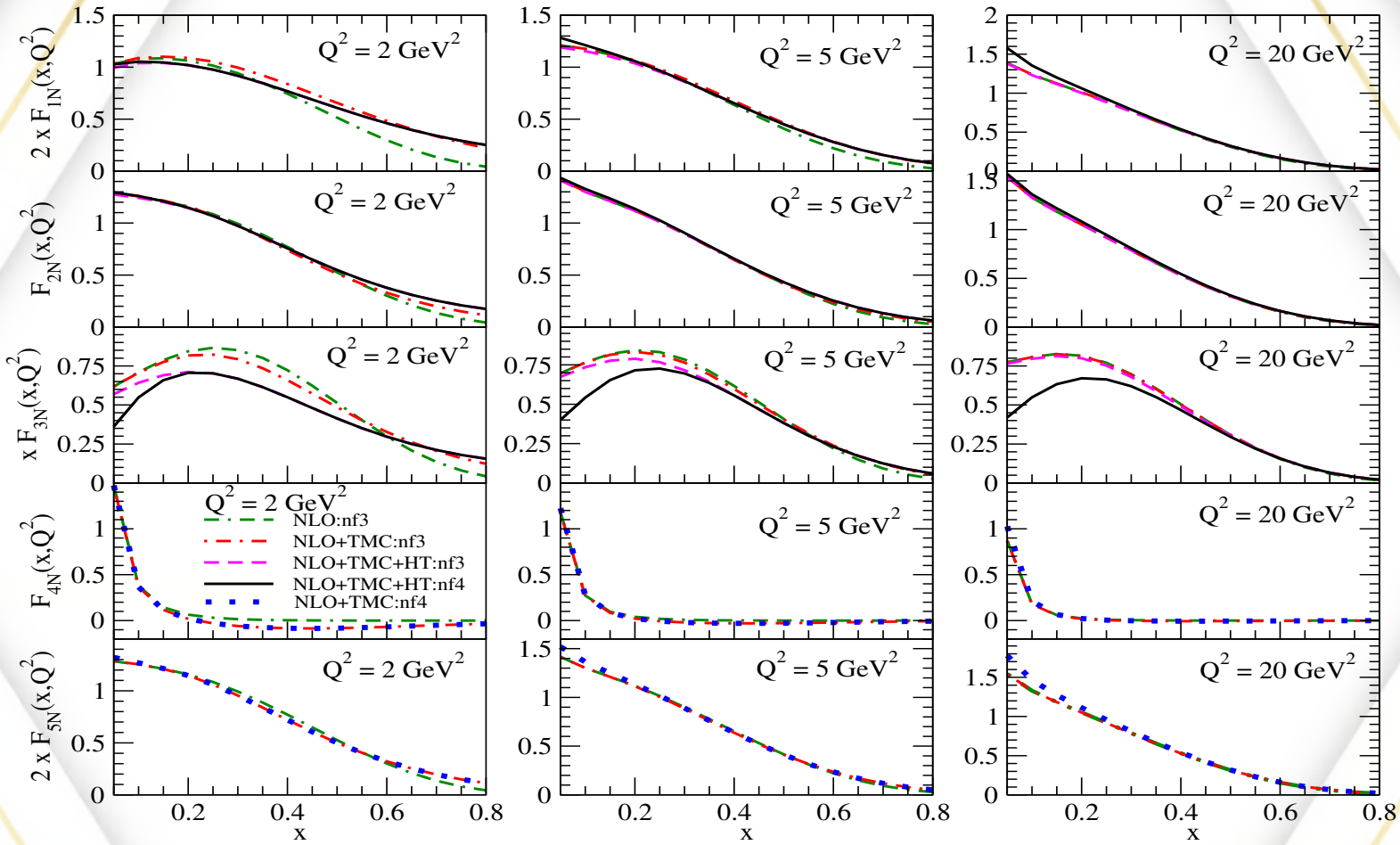

Figure: Results for free nucleon structure functions $F_{iN}(x,Q^2);(i=1-5)$ at different values of Q^2 are shown.

Phys. Rev. D.102 (2020) 11, 113007

Ratio of $\frac{\sigma_{\nu\tau}}{\sigma_{\nu\mu}}$ vs E for free nucleon

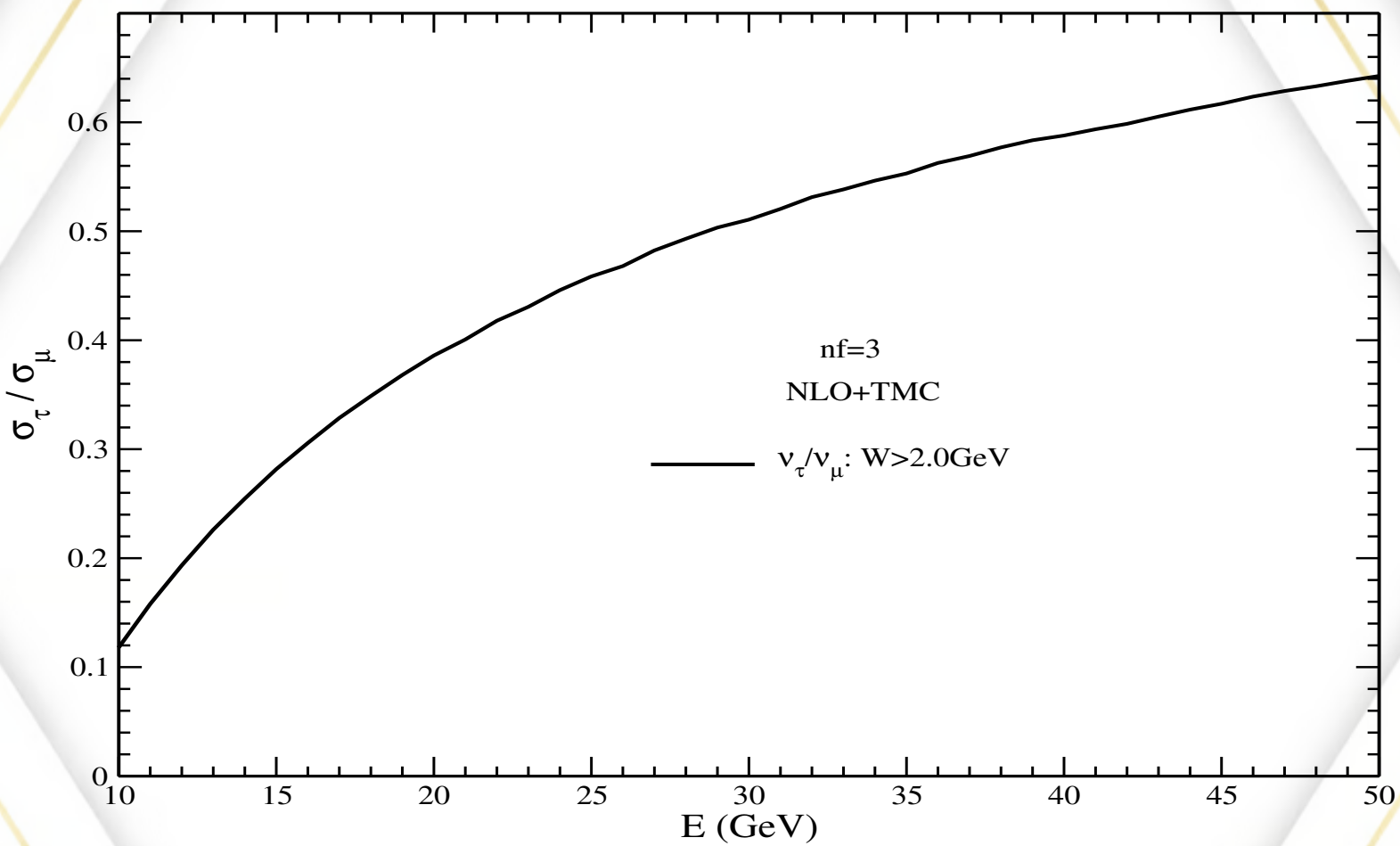

Figure: Ratio of the total scattering cross section $\frac{\sigma_{\nu\tau}}{\sigma_{\nu\mu}}$ vs E with $W > 2$ GeV for tau type (anti)neutrinos are shown.

Phys. Rev. D.102 (2020) 11, 113007

Ratio of $\frac{\sigma_{\nu\tau}}{\sigma_{\nu\mu}}$ vs E for free nucleon

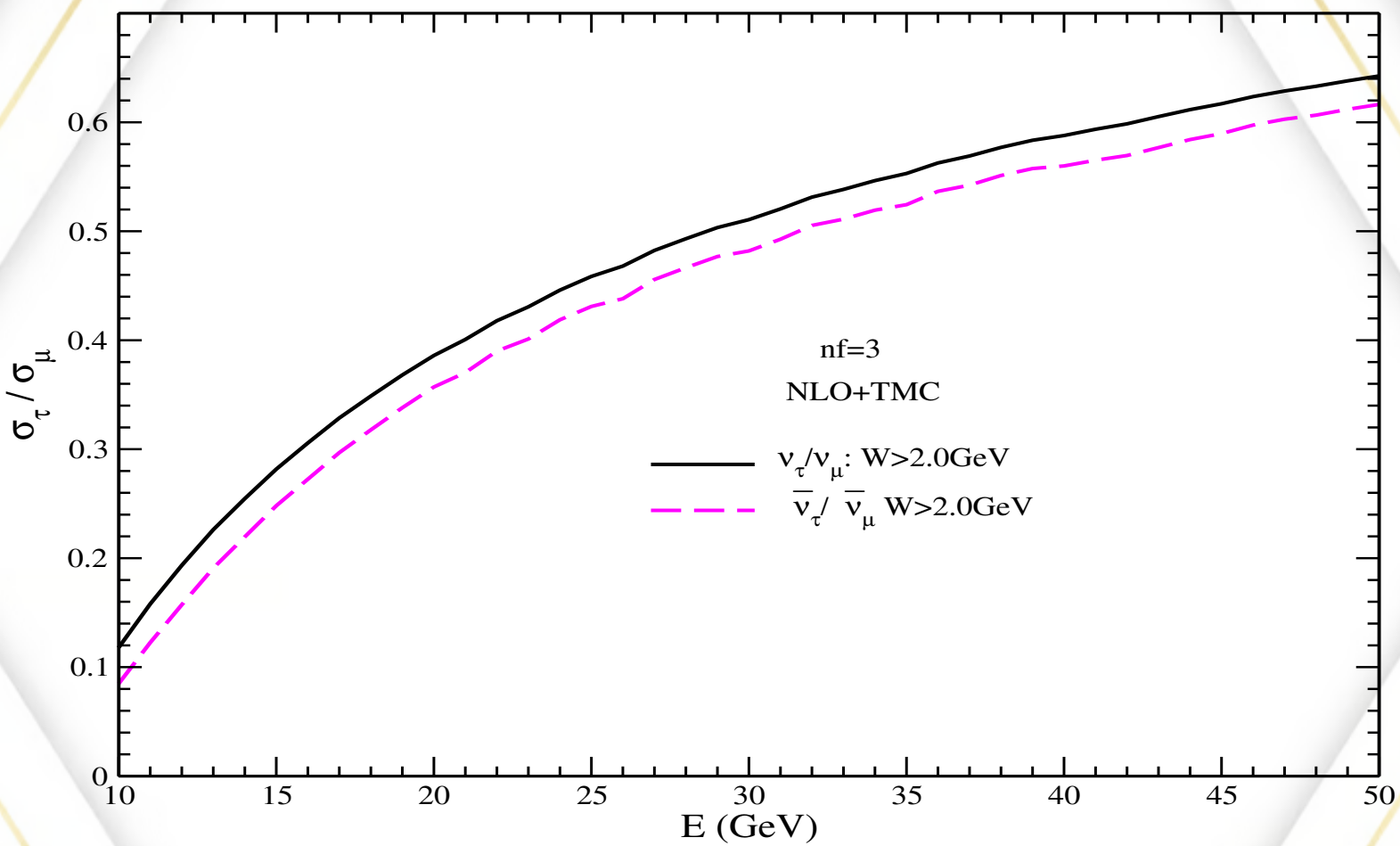

Figure: Ratio of the total scattering cross section $\frac{\sigma_{\nu\tau}}{\sigma_{\nu\mu}}$ vs E with $W > 2$ GeV for tau type (anti)neutrinos are shown.

Phys. Rev. D.102 (2020) 11, 113007

$\nu_\tau - A$ DIS

$$\nu_\tau(k) + A(p) \rightarrow \tau^-(k') + X(p')$$

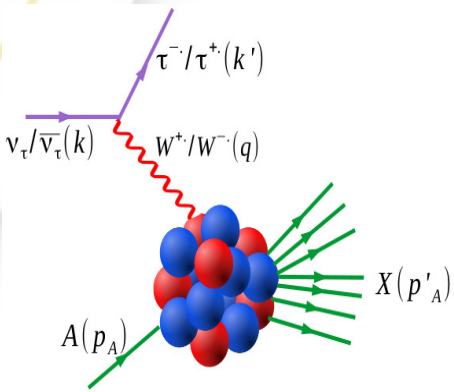

$\nu_\tau - A$ DIS

$$\nu_\tau(k) + A(p) \rightarrow \tau^-(k') + X(p')$$

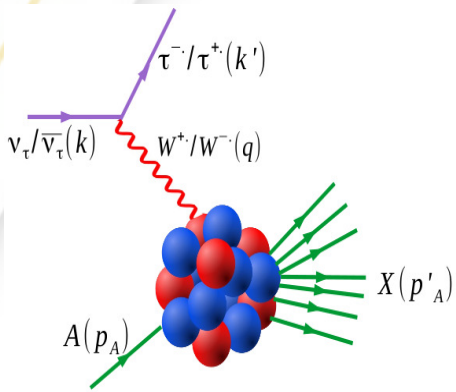

The differential scattering cross section for neutrino induced DIS process off nuclear target is given by:

$$\frac{d^2\sigma_A}{dxdy} = \frac{G_F^2 y}{16\pi}\left(\frac{M_W^2}{Q^2+M_W^2}\right)^2 L^{\alpha\beta} W^A_{\alpha\beta},$$

$\nu_\tau - A$ DIS

$$\nu_\tau(k) + A(p) \to \tau^-(k') + X(p')$$

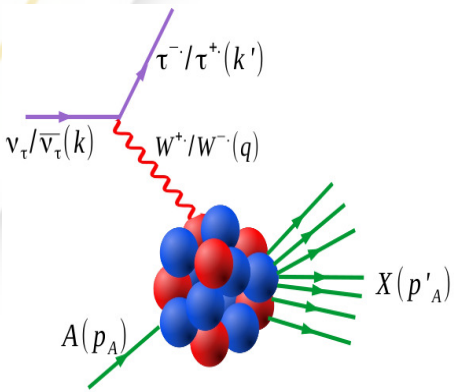

The differential scattering cross section for neutrino induced DIS process off nuclear target is given by:

$$\frac{d^2\sigma_A}{dxdy} = \frac{G_F^2 y}{16\pi}\left(\frac{M_W^2}{Q^2+M_W^2}\right)^2 L^{\alpha\beta} W^A_{\alpha\beta}, \quad W^N_{\alpha\beta} \to W^A_{\alpha\beta}$$

$\nu_\tau - A$ DIS

$$\nu_\tau(k) + A(p) \to \tau^-(k') + X(p')$$

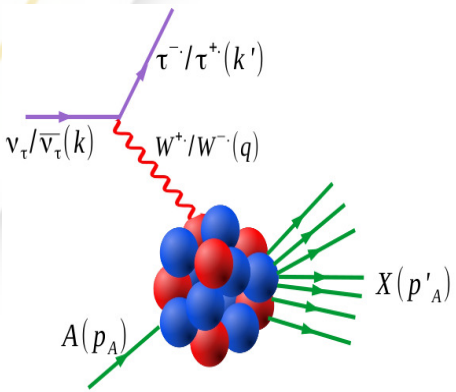

The differential scattering cross section for neutrino induced DIS process off nuclear target is given by:

$$\frac{d^2\sigma_A}{dxdy} = \frac{G_F^2 y}{16\pi}\left(\frac{M_W^2}{Q^2+M_W^2}\right)^2 L^{\alpha\beta} W^A_{\alpha\beta}, \quad W^N_{\alpha\beta} \to W^A_{\alpha\beta}$$

The nuclear hadronic tensor is written in terms of dimensionless nuclear structure functions $F_{iA}(x,Q^2)$ as:

$$\begin{aligned} W^A_{\alpha\beta} &= -g_{\alpha\beta}F_{1A}(x,Q^2) + \frac{p_\alpha p_\beta}{p\cdot q}F_{2A}(x,Q^2) - \frac{i}{2p\cdot q}\varepsilon_{\alpha\beta\rho\sigma}p^\rho q^\sigma \\ &\times F_{3A}(x,Q^2) + \frac{q_\alpha q_\beta}{p\cdot q}F_{4A}(x,Q^2) + (p_\alpha q_\beta + p_\beta q_\alpha)F_{5A}(x,Q^2). \end{aligned}$$

where $F_{iA}(x,Q^2)$; $i = 1-5$ are the nuclear structure functions.

$\nu_\tau - A$ DIS

$$\nu_\tau(k) + A(p) \to \tau^-(k') + X(p')$$

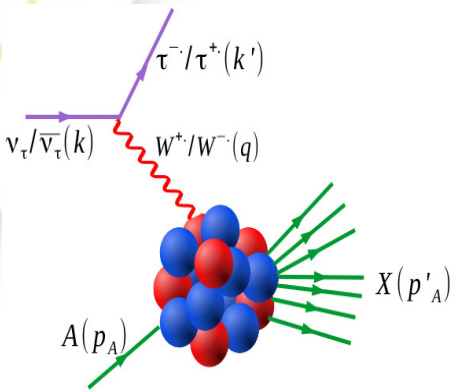

The differential scattering cross section for neutrino induced DIS process off nuclear target is given by:

$$\frac{d^2\sigma_A}{dxdy} = \frac{G_F^2 y}{16\pi}\left(\frac{M_W^2}{Q^2+M_W^2}\right)^2 L^{\alpha\beta} W^A_{\alpha\beta}, \quad W^N_{\alpha\beta} \to W^A_{\alpha\beta}$$

The nuclear hadronic tensor is written in terms of dimensionless nuclear structure functions $F_{iA}(x,Q^2)$ as:

$$\begin{aligned} W^A_{\alpha\beta} &= -g_{\alpha\beta}F_{1A}(x,Q^2) + \frac{p_\alpha p_\beta}{p\cdot q}F_{2A}(x,Q^2) - \frac{i}{2p\cdot q}\varepsilon_{\alpha\beta\rho\sigma}p^\rho q^\sigma \\ &\times F_{3A}(x,Q^2) + \frac{q_\alpha q_\beta}{p\cdot q}F_{4A}(x,Q^2) + (p_\alpha q_\beta + p_\beta q_\alpha)F_{5A}(x,Q^2). \end{aligned}$$

where $F_{iA}(x,Q^2)$; $i = 1-5$ are the nuclear structure functions.

Following NME are incorporated (Phys. Rev. D.105 (2022) 3, 033010):

- Fermi motion, binding energy and nucleon correlations through spectral function.

$\nu_\tau - A$ DIS

$$\nu_\tau(k) + A(p) \to \tau^-(k') + X(p')$$

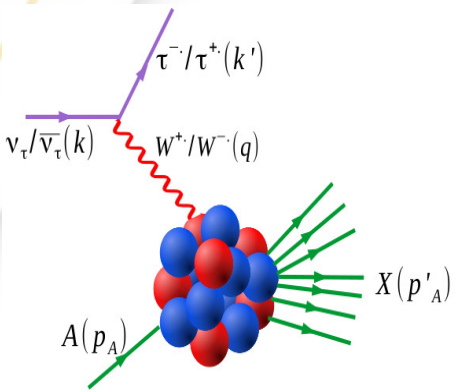

The differential scattering cross section for neutrino induced DIS process off nuclear target is given by:

$$\frac{d^2\sigma_A}{dxdy} = \frac{G_F^2 y}{16\pi}\left(\frac{M_W^2}{Q^2+M_W^2}\right)^2 L^{\alpha\beta} W^A_{\alpha\beta}, \quad W^N_{\alpha\beta} \to W^A_{\alpha\beta}$$

The nuclear hadronic tensor is written in terms of dimensionless nuclear structure functions $F_{iA}(x,Q^2)$ as:

$$\begin{aligned} W^A_{\alpha\beta} &= -g_{\alpha\beta}F_{1A}(x,Q^2) + \frac{p_\alpha p_\beta}{p\cdot q}F_{2A}(x,Q^2) - \frac{i}{2p\cdot q}\varepsilon_{\alpha\beta\rho\sigma}p^\rho q^\sigma \\ &\times F_{3A}(x,Q^2) + \frac{q_\alpha q_\beta}{p\cdot q}F_{4A}(x,Q^2) + (p_\alpha q_\beta + p_\beta q_\alpha)F_{5A}(x,Q^2). \end{aligned}$$

where $F_{iA}(x,Q^2)$; $i = 1-5$ are the nuclear structure functions.

Following NME are incorporated (Phys. Rev. D.105 (2022) 3, 033010):

- Fermi motion, binding energy and nucleon correlations through spectral function.
- The spectral functions has been calculated using Lehmann's representation for the relativistic nucleon propagator.

$\nu_\tau - A$ DIS

$$\nu_\tau(k) + A(p) \to \tau^-(k') + X(p')$$

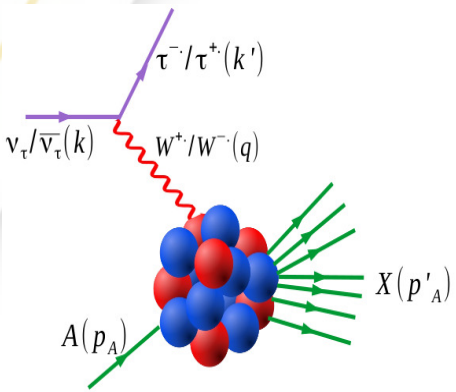

The differential scattering cross section for neutrino induced DIS process off nuclear target is given by:

$$\frac{d^2\sigma_A}{dxdy} = \frac{G_F^2 y}{16\pi}\left(\frac{M_W^2}{Q^2+M_W^2}\right)^2 L^{\alpha\beta} W^A_{\alpha\beta}, \quad W^N_{\alpha\beta} \to W^A_{\alpha\beta}$$

The nuclear hadronic tensor is written in terms of dimensionless nuclear structure functions $F_{iA}(x,Q^2)$ as:

$$\begin{aligned} W^A_{\alpha\beta} &= -g_{\alpha\beta}F_{1A}(x,Q^2) + \frac{p_\alpha p_\beta}{p\cdot q}F_{2A}(x,Q^2) - \frac{i}{2p\cdot q}\varepsilon_{\alpha\beta\rho\sigma}p^\rho q^\sigma \\ &\times F_{3A}(x,Q^2) + \frac{q_\alpha q_\beta}{p\cdot q}F_{4A}(x,Q^2) + (p_\alpha q_\beta + p_\beta q_\alpha)F_{5A}(x,Q^2). \end{aligned}$$

where $F_{iA}(x,Q^2)$; $i = 1-5$ are the nuclear structure functions.

Following NME are incorporated (Phys. Rev. D.105 (2022) 3, 033010):

- Fermi motion, binding energy and nucleon correlations through spectral function.
- The spectral functions has been calculated using Lehmann's representation for the relativistic nucleon propagator.
- Nuclear many body theory is used to calculate it for an interacting Fermi sea in nuclear matter (Marco et al., NPA 611, 484 (1996); Fernandez de Cordoba et al., PRC 46, 1697(1992)).

$\nu_\tau - A$ DIS

$$\nu_\tau(k) + A(p) \to \tau^-(k') + X(p')$$

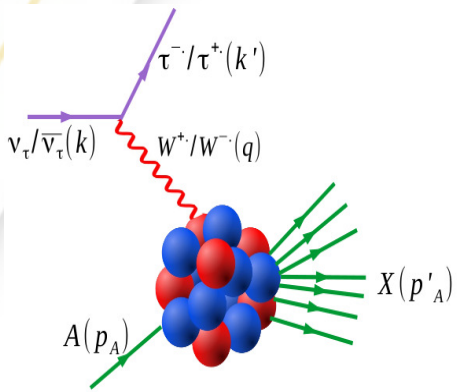

The differential scattering cross section for neutrino induced DIS process off nuclear target is given by:

$$\frac{d^2\sigma_A}{dxdy} = \frac{G_F^2 y}{16\pi}\left(\frac{M_W^2}{Q^2+M_W^2}\right)^2 L^{\alpha\beta} W^A_{\alpha\beta}, \quad W^N_{\alpha\beta} \to W^A_{\alpha\beta}$$

The nuclear hadronic tensor is written in terms of dimensionless nuclear structure functions $F_{iA}(x,Q^2)$ as:

$$\begin{aligned} W^A_{\alpha\beta} &= -g_{\alpha\beta}F_{1A}(x,Q^2) + \frac{p_\alpha p_\beta}{p\cdot q}F_{2A}(x,Q^2) - \frac{i}{2p\cdot q}\varepsilon_{\alpha\beta\rho\sigma}p^\rho q^\sigma \\ &\times F_{3A}(x,Q^2) + \frac{q_\alpha q_\beta}{p\cdot q}F_{4A}(x,Q^2) + (p_\alpha q_\beta + p_\beta q_\alpha)F_{5A}(x,Q^2). \end{aligned}$$

where $F_{iA}(x,Q^2)$; $i = 1-5$ are the nuclear structure functions.

Following NME are incorporated (Phys. Rev. D.105 (2022) 3, 033010):

- Fermi motion, binding energy and nucleon correlations through spectral function.
- The spectral functions has been calculated using Lehmann's representation for the relativistic nucleon propagator.
- Nuclear many body theory is used to calculate it for an interacting Fermi sea in nuclear matter (Marco et al., NPA 611, 484 (1996); Fernandez de Cordoba et al., PRC 46, 1697(1992)).
- Pion and rho meson cloud contributions following the many body field theoretical approach (Marco et al., NPA 611, 484 (1996)).

$\nu_\tau - A$ DIS

$$\nu_\tau(k) + A(p) \to \tau^-(k') + X(p')$$

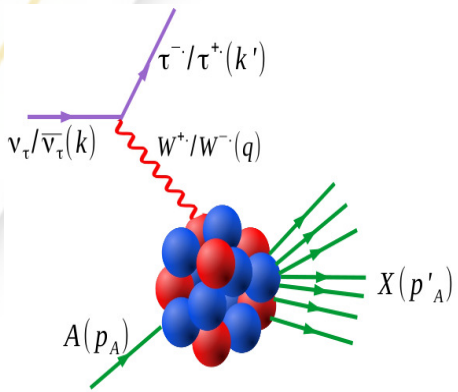

The differential scattering cross section for neutrino induced DIS process off nuclear target is given by:

$$\frac{d^2\sigma_A}{dxdy} = \frac{G_F^2 y}{16\pi}\left(\frac{M_W^2}{Q^2+M_W^2}\right)^2 L^{\alpha\beta} W^A_{\alpha\beta}, \quad W^N_{\alpha\beta} \to W^A_{\alpha\beta}$$

The nuclear hadronic tensor is written in terms of dimensionless nuclear structure functions $F_{iA}(x,Q^2)$ as:

$$\begin{aligned} W^A_{\alpha\beta} &= -g_{\alpha\beta}F_{1A}(x,Q^2) + \frac{p_\alpha p_\beta}{p\cdot q}F_{2A}(x,Q^2) - \frac{i}{2p\cdot q}\varepsilon_{\alpha\beta\rho\sigma}p^\rho q^\sigma \\ &\times F_{3A}(x,Q^2) + \frac{q_\alpha q_\beta}{p\cdot q}F_{4A}(x,Q^2) + (p_\alpha q_\beta + p_\beta q_\alpha)F_{5A}(x,Q^2). \end{aligned}$$

where $F_{iA}(x,Q^2)$; $i = 1-5$ are the nuclear structure functions.

Following NME are incorporated (Phys. Rev. D.105 (2022) 3, 033010):

- Fermi motion, binding energy and nucleon correlations through spectral function.
- The spectral functions has been calculated using Lehmann's representation for the relativistic nucleon propagator.
- Nuclear many body theory is used to calculate it for an interacting Fermi sea in nuclear matter (Marco et al., NPA 611, 484 (1996); Fernandez de Cordoba et al., PRC 46, 1697(1992)).
- Pion and rho meson cloud contributions following the many body field theoretical approach (Marco et al., NPA 611, 484 (1996)).
- Shadowing and antishadowing effects following the works of Kulagin and Petti (PRD **76**, 094033 (2007)).

Formalism

The DCX for ν_l-N scattering is

$$d\sigma = \Gamma\, dt\, dS$$

- Probability per unit time
- Time of interaction
- Differential area

We may write it as

$$d\sigma = \Gamma \frac{dt}{dl} dS\, dl = \Gamma \frac{1}{v} d^3r = \Gamma \frac{E(k)}{|k|} d^3r$$

- Length of interaction
- Velocity of lepton

$$f = \frac{1}{k^0 - E(k) + i\frac{\Gamma}{2}}$$

$$G(k^0,k) = \sum_r \frac{\bar{u}_r(k')u_r(k)}{k^0 - E(k) - \frac{m_l}{E}\bar{u}_r(k')\Sigma(k)u_r(k)}$$

$$G(k^0,k) = \sum_r \frac{\bar{u}_r(k')u_r(k)}{k^0 - E(k) - \frac{m_l}{E}\bar{u}_r(k')(\Re\Sigma(k) + i\Im\Sigma(k))u_r(k)}$$

$$\Gamma = \frac{-2m_l}{E(k)} Im\,\Sigma(k)$$

$$d\sigma = \frac{-2m_l}{|k|} Im\,\Sigma(k)\, d^3r$$

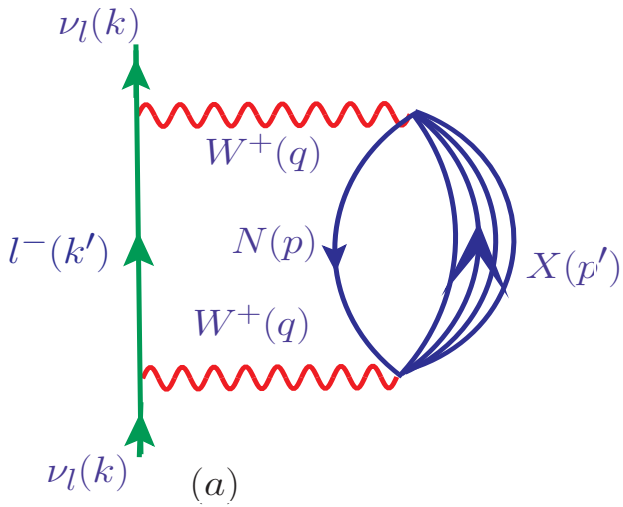
$\nu_l(k)$
$W^+(q)$
$l^-(k')$
$N(p)$
$X(p')$
$W^+(q)$
$\nu_l(k)$
(a)

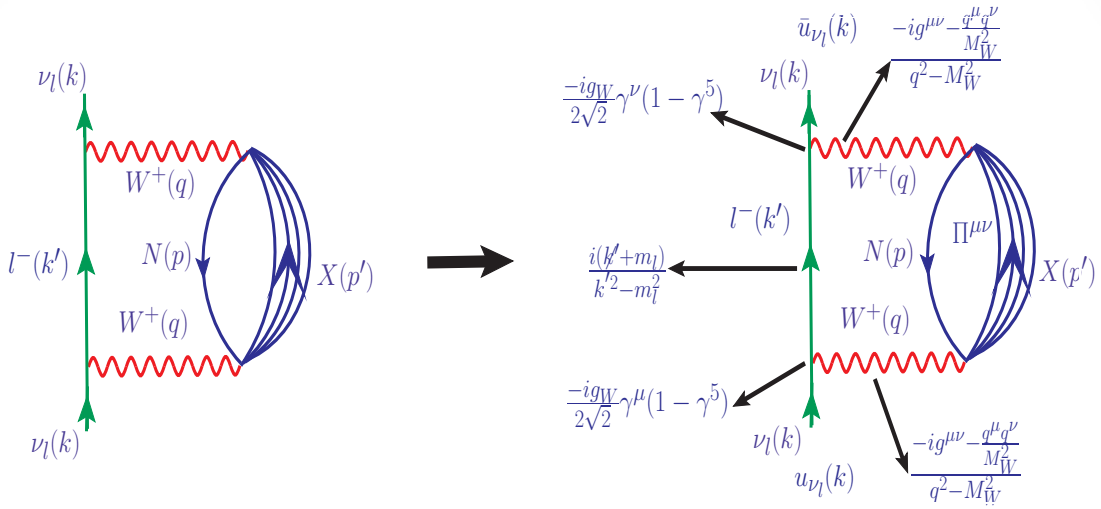

- Neutrino self energy $\Sigma(k)$:

$$\Sigma(k) \quad = \quad \frac{iG_F}{\sqrt{2}} \int \frac{d^4q}{(2\pi)^4} \frac{4L^{WI}_{\mu\nu}}{m_l} \frac{1}{(k'^2 - m_l^2 + i\varepsilon)} \left(\frac{M_W}{q^2 - M_W^2} \right)^2 \Pi^{\mu\nu}(q) \,,$$

- Imaginary part of neutrino self energy:

$$Im\Sigma(k) = \frac{G_F}{\sqrt{2}} \frac{4}{m_\nu} \int \frac{d^3k'}{(2\pi)^4} \frac{\pi}{E(\mathbf{k}')} \theta(q^0) \left(\frac{M_W}{Q^2 + M_W^2} \right)^2 Im[L^{WI}_{\mu\nu} \Pi^{\mu\nu}(q)]$$

$W-$boson self energy

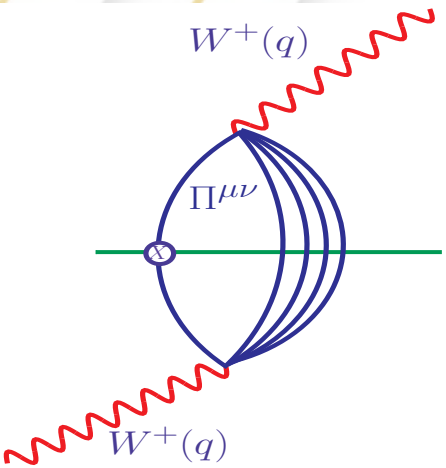

$$\Pi^{\mu\nu}(q) = \left(\frac{G_F M_W^2}{\sqrt{2}}\right) \times \int \frac{d^4p}{(2\pi)^4} G(p) \sum_X \sum_{sp,s_l} \prod_{i=1}^{N} \int \frac{d^4p_i'}{(2\pi)^4} \prod_l G_l(p_l')$$

$$\times \prod_j D_j(p_j') < X|J^\mu|N >< X|J^\nu|N >^* (2\pi)^4$$

$$\times \delta^4(k+p-k'-\sum_{i=1}^{N} p_i'),$$

$W-$boson self energy

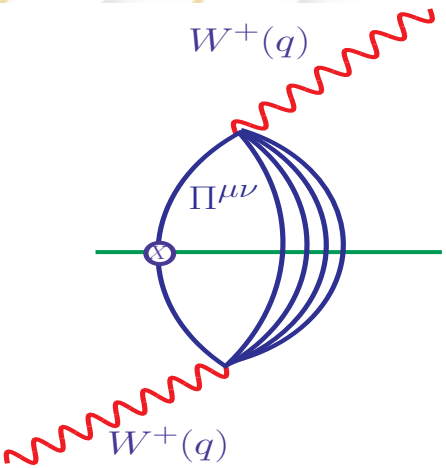

$$\Pi^{\mu\nu}(q) = \left(\frac{G_F M_W^2}{\sqrt{2}}\right) \times \int \frac{d^4p}{(2\pi)^4} G(p) \sum_X \sum_{s_p, s_l} \prod_{i=1}^{N} \int \frac{d^4p_i'}{(2\pi)^4} \prod_l G_l(p_l')$$
$$\times \prod_j D_j(p_j') < X|J^\mu|N >< X|J^\nu|N >^* (2\pi)^4$$
$$\times \delta^4(k+p-k'-\sum_{i=1}^{N} p_i'),$$

- Relativistic nucleon propagator in the nuclear medium:

$$G(p^0, \mathbf{p}) = \frac{M}{E(\mathbf{p})} \sum_r u_r(\mathbf{p}) \bar{u}_r(\mathbf{p}) \left[\int_{-\infty}^{\mu} d\omega \frac{S_h(\omega, \mathbf{p})}{p^0 - \omega - i\varepsilon} + \int_{\mu}^{\infty} d\omega \frac{S_p(\omega, \mathbf{p})}{p^0 - \omega + i\varepsilon} \right]$$

- For $p^0 \leq \mu$

$$S_h(p^0, \mathbf{p}) = \frac{1}{\pi} \frac{\frac{M}{E(\mathbf{p})} Im\Sigma(p^0, \mathbf{p})}{(p^0 - E(\mathbf{p}) - \frac{M}{E(\mathbf{p})} Re\Sigma(p^0, \mathbf{p}))^2 + (\frac{M}{E(\mathbf{p})} Im\Sigma(p^0, \mathbf{p}))^2}$$

- For $p^0 > \mu$

$$S_p(p^0, \mathbf{p}) = -\frac{1}{\pi} \frac{\frac{M}{E(\mathbf{p})} Im\Sigma(p^0, \mathbf{p})}{(p^0 - E(\mathbf{p}) - \frac{M}{E(\mathbf{p})} Re\Sigma(p^0, \mathbf{p}))^2 + (\frac{M}{E(\mathbf{p})} Im\Sigma(p^0, \mathbf{p}))^2}$$

We evaluate dimensionless nuclear structure functions in terms of hole spectral function and free nucleon structure functions:

$$F_{iA,N}(x_A, Q^2) = 4 \int d^3r \int \frac{d^3p}{(2\pi)^3} \frac{M_N}{E_N(\mathbf{p})} \int_{-\infty}^{\mu} dp^0 \, S_h(p^0, \mathbf{p}, \rho(r)) \times f_{iN}(x, Q^2)$$

For example,

$$f_{1N}(x, Q^2) = AM_N \left[\frac{F_{1N}(x_N, Q^2)}{M_N} + \left(\frac{p^x}{M_N} \right)^2 \frac{F_{2N}(x_N, Q^2)}{\nu_N} \right],$$

$$f_{2N}(x, Q^2) = \left(\frac{F_{2N}(x_N, Q^2)}{M_N^2 \nu_N} \right) \left[\frac{Q^4}{q^0 (q^z)^2} \left(p^z + \frac{q^0 (p^0 - \gamma p^z)}{Q^2} q^z \right)^2 + \frac{q^0 Q^2 (p^x)^2}{(q^z)^2} \right]$$

$$f_{3N}(x, Q^2) = A \frac{q^0}{q^z} \times \left(\frac{p^0 q^z - p^z q^0}{p \cdot q} \right) F_{3N}(x_N, Q^2),$$

$$f_{4N}(x, Q^2) = A \left[F_{4N}(x_N, Q^2) + \frac{p^z Q^2}{q^z} \frac{F_{5N}(x, Q^2)}{M_N \nu_N} \right],$$

$$f_{5N}(x, Q^2) = A \frac{F_{5N}(x_N, Q^2)}{M_N \nu_N} \times \left[q^0 (p^0 - \gamma p^z) + Q^2 \frac{p^z}{q^z} \right]$$

π and ρ mesons contribution

- Nucleons interact among themselves via the exchange of virtual mesons.

π and ρ mesons contribution

- Nucleons interact among themselves via the exchange of virtual mesons.
- $\mathscr{P}^{\gamma^*}_{meson}$ increases instead the $\mathscr{P}^{\gamma^*}_{nucleon}$.

π and ρ mesons contribution

- Nucleons interact among themselves via the exchange of virtual mesons.
- $\mathscr{P}^{\gamma^*}_{meson}$ increases instead the $\mathscr{P}^{\gamma^*}_{nucleon}$.
- Contributions from π and ρ mesons have been incorporated.

π and ρ mesons contribution

- Nucleons interact among themselves via the exchange of virtual mesons.
- $\mathscr{P}^{\gamma^*}_{meson}$ increases instead the $\mathscr{P}^{\gamma^*}_{nucleon}$.
- Contributions from π and ρ mesons have been incorporated.
- Implemented following the many body field theoretical approach.

π and ρ mesons contribution

- Nucleons interact among themselves via the exchange of virtual mesons.
- $\mathscr{P}^{\gamma^*}_{meson}$ increases instead the $\mathscr{P}^{\gamma^*}_{nucleon}$.
- Contributions from π and ρ mesons have been incorporated.
- Implemented following the many body field theoretical approach.
- For pion PDFs parameterization by Gluck et al. has been used.

$$F_{iA,a}(x,Q^2) \quad = \quad -6\kappa \int d^3r \int \frac{d^4p}{(2\pi)^4}\theta(p^0)\ \delta ImD_a(p)\ 2m_a\ f_{ia}(x_a),$$

where

- $i = 1,2,5$; $a = \pi,\rho$; $\kappa = 1$ for pion and $\kappa = 2$ for rho meson.
- $D_a(p)$ is the dressed meson propagator.
- $x_a = -\frac{Q^2}{2p\cdot q}$.
- f_{ia} is the pionic structure functions.
- No mesonic cloud contribution in $F_{3A}(x,Q^2)$ and $F_{4A}(x,Q^2)$.

Shadowing and Antishadowing effects

"Shadowing and antishadowing effects arises due to the destructive and constructive interference of amplitudes arises from the multiple scattering of quarks/antiquarks inside the nucleus."

- Significant at low-x and low-Q^2.
- The ratio $\frac{F_{2A}(x,Q^2)}{F_{2N}(x,Q^2)}$ suppressed due to shadowing.
- However, antishadowing enhance this ratio.
- We incorporate it following the works of Kulagin and Petti(PRD **76**, 094023 (2007)).
- We define

$$F_{iA,shd}(x,Q^2) = \delta R_i(x,Q^2) \times F_{i,N}(x,Q^2),$$

  where $\delta R_i(x,Q^2)$ is the shadowing correction factor.
- Shadowing effect is not known for $F_{4A}(x,Q^2)$.
- Shadowing effect is also not known explicitly for $F_{5A}(x,Q^2)$, but here we have included it by using the Albright-Jarlskog relation.

Nuclear medium effects considered by AMU group:

Nuclear medium effects considered by AMU group:

- Fermi motion
- Binding energy
- Nucleon correlations

} Spectral function (SF)

} $SF+\pi+\rho$

- Mesonic contributions
- Shadowing and antishadowing corrections

} Total

Nuclear structure functions: F_{1A}, F_{2A} and F_{3A} vs x in ^{40}Ar

In the theoretical model with spectral function only:

$$F_{iA}(x,Q^2) = F_{iA,N}(x,Q^2)\ ;\ i = 1-3$$

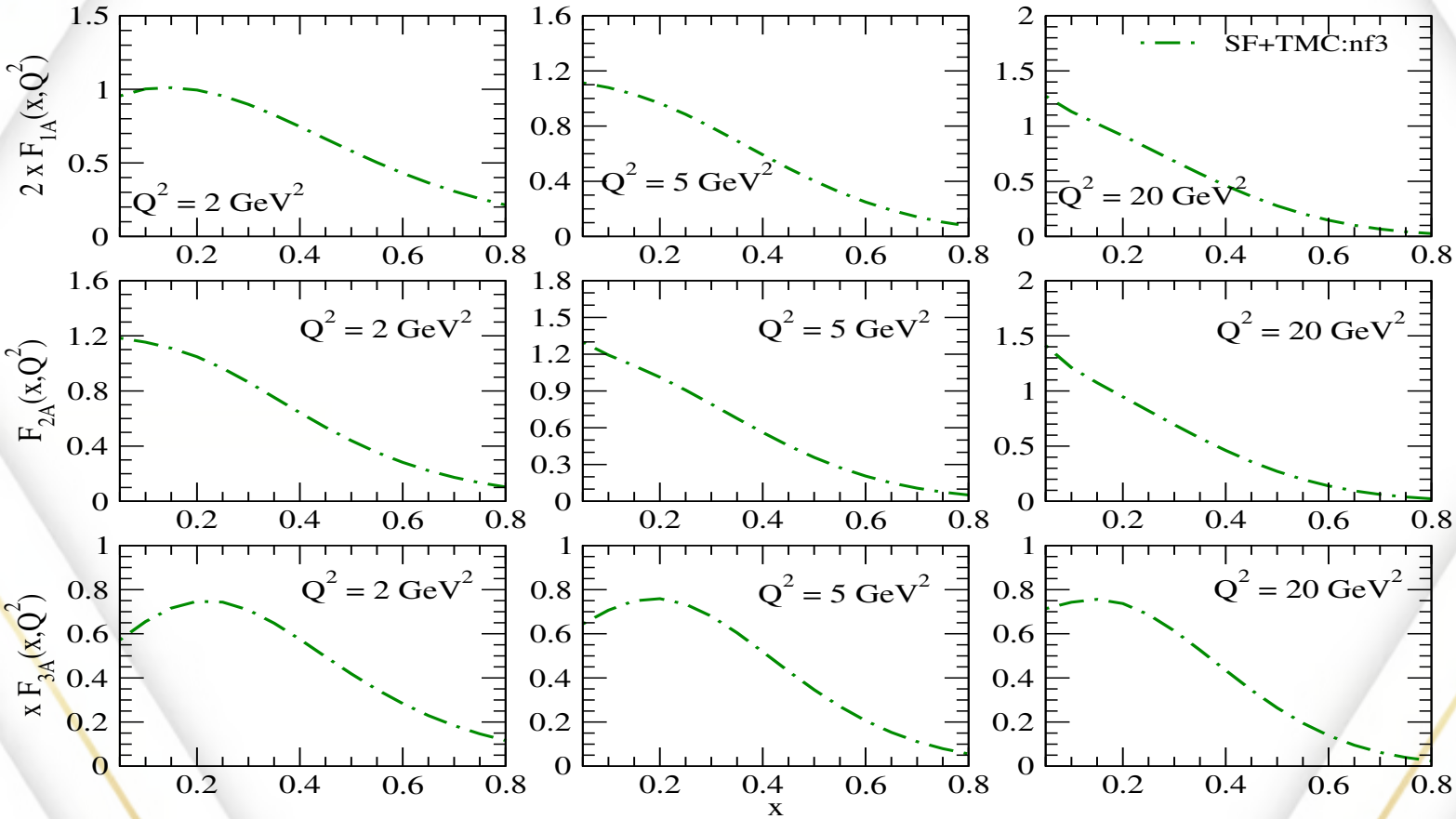

Phys. Rev. D.105 (2022) 3, 033010

Nuclear structure functions: F_{1A}, F_{2A} and F_{3A} vs x in ^{40}Ar

In the theoretical model with spectral function only:

$$F_{iA}(x,Q^2) = F_{iA,N}(x,Q^2)\ ;\ i = 1-3$$

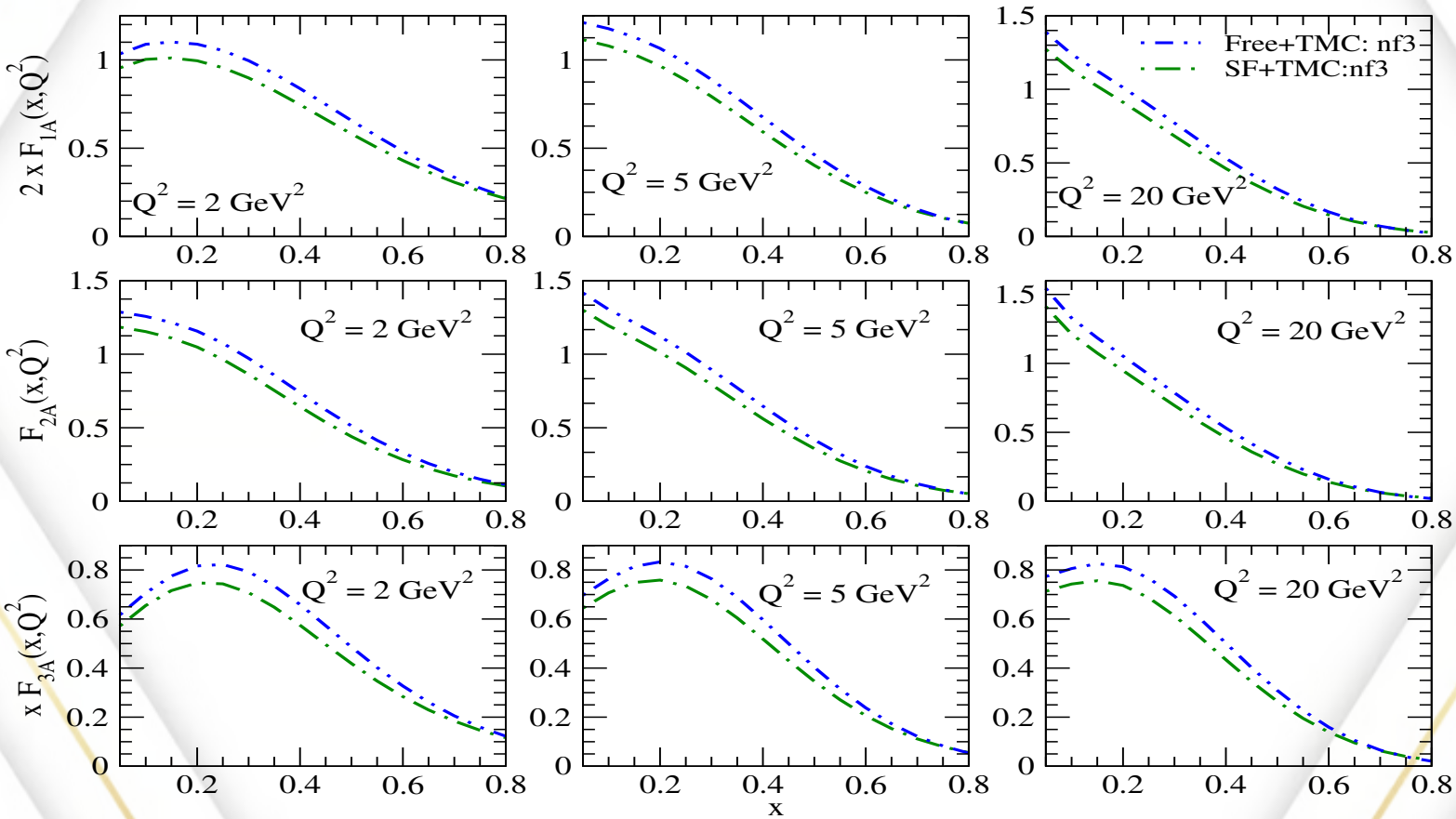

Phys. Rev. D.105 (2022) 3, 033010

Nuclear structure functions: F_{1A}, F_{2A} and F_{3A} vs x in ^{40}Ar

In the theoretical model with spectral function only:

$$F_{iA}(x,Q^2) = F_{iA,N}(x,Q^2)\ ;\ i = 1-3$$

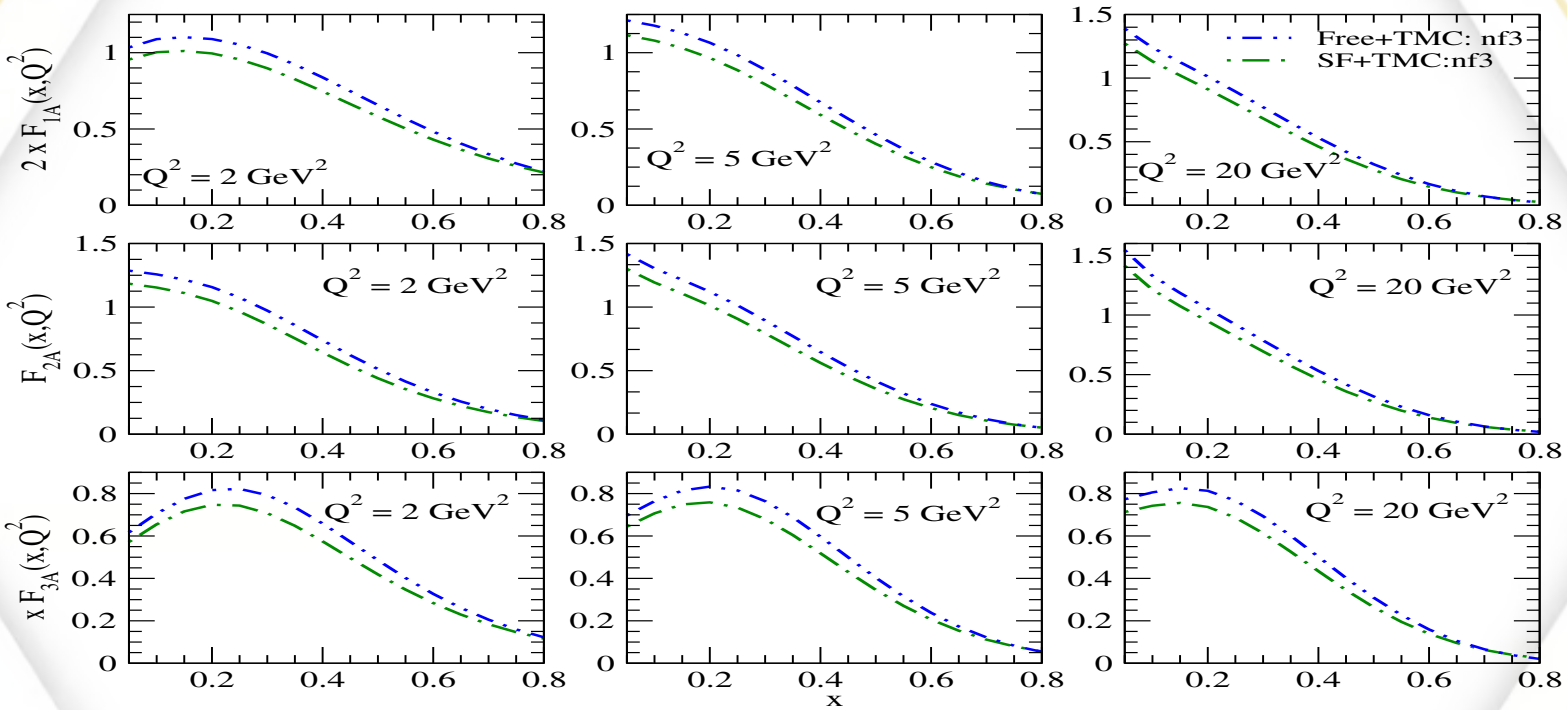

$Q^2(GeV^2)$	x	$(Free - SF) * 100/Free$		
		$F_{1A}(x,Q^2)$	$F_{2A}(x,Q^2)$	$F_{3A}(x,Q^2)$
2	0.1	8%	8%	7%
	0.25	9%	10%	$\approx$ 10%
	0.5	11%	14%	13%

Nuclear structure functions: F_{1A}, F_{2A} and F_{3A} vs x in ^{40}Ar

In the full theoretical model:

$$F_{iA}(x,Q^2) = F_{iA,N}(x,Q^2) + F_{iA,\pi}(x,Q^2) + F_{iA,\rho}(x,Q^2) + F_{iA,shd}(x,Q^2);\ \ i = 1-2$$

$$F_{3A}(x,Q^2) = F_{3A,N}(x,Q^2) + F_{3A,shd}(x,Q^2)$$

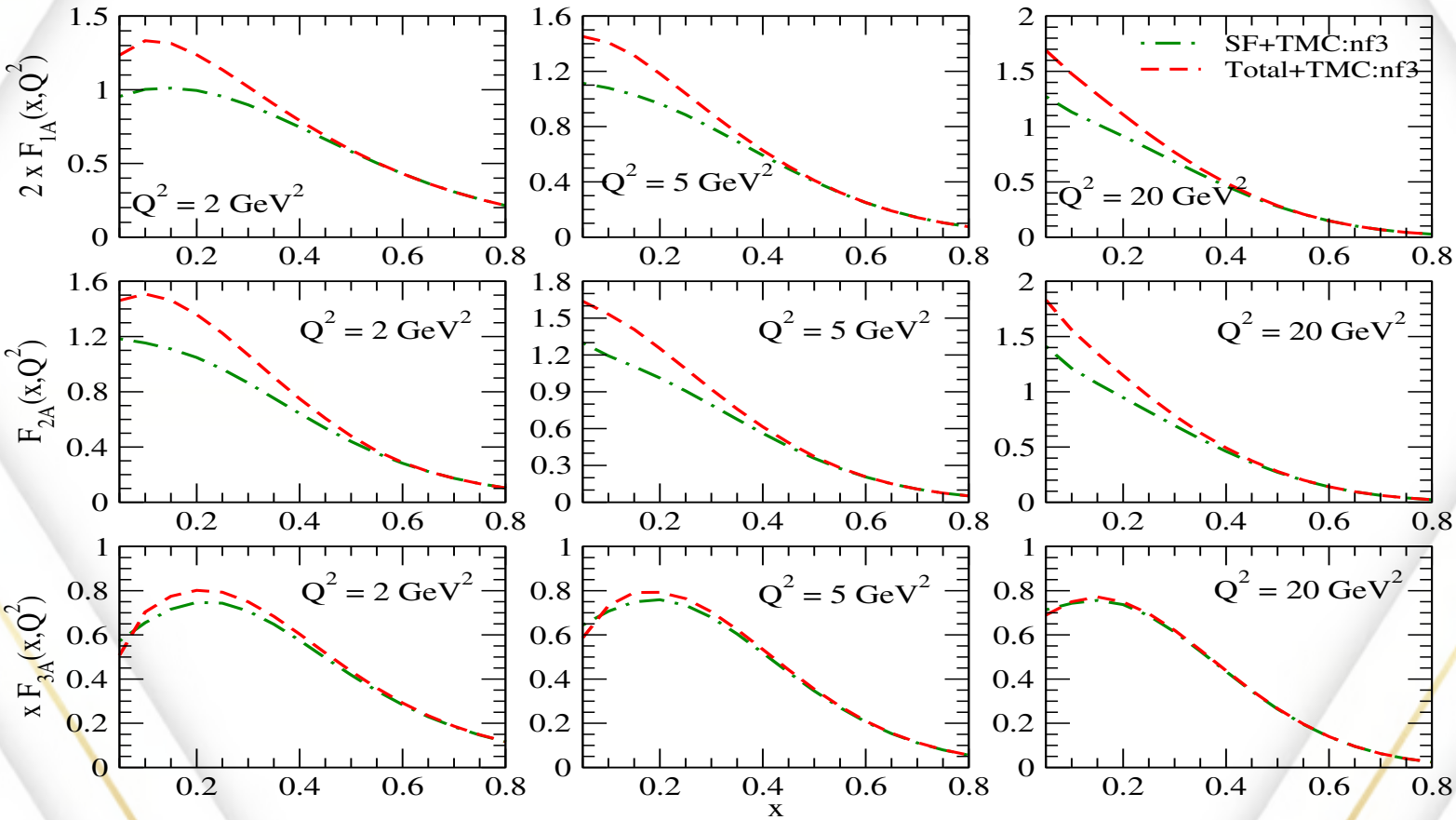

Phys. Rev. D.105 (2022) 3, 033010

Nuclear structure functions: F_{1A}, F_{2A} and F_{3A} vs x in ^{40}Ar

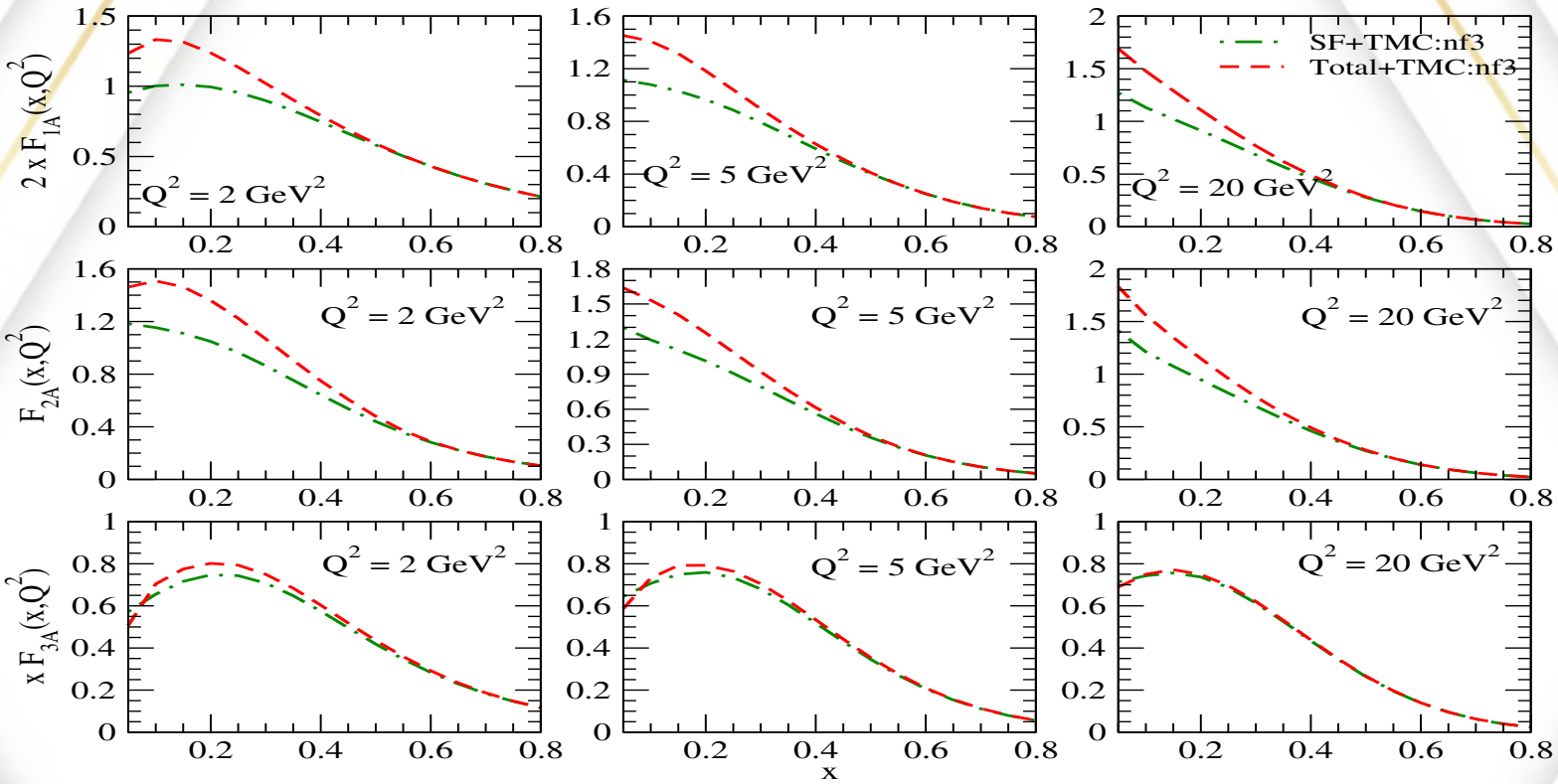

$Q^2(GeV^2)$	x	$(Total-SF)*100/SF$		
		$F_{1A}(x,Q^2)$	$F_{2A}(x,Q^2)$	$F_{3A}(x,Q^2)$
2	0.1	33%	31%	7%
	0.25	19%	27%	5%
	0.5	2%	9%	4%

Phys. Rev. D.105 (2022) 3, 033010

Nuclear structure functions: F_{1A}, F_{2A} and F_{3A} vs x in ^{40}Ar

In the full theoretical model:

$$F_{iA}(x,Q^2) = F_{iA,N}(x,Q^2) + F_{iA,\pi}(x,Q^2) + F_{iA,\rho}(x,Q^2) + F_{iA,shd}(x,Q^2);\ \ i = 1-2$$

$$F_{3A}(x,Q^2) = F_{3A,N}(x,Q^2) + F_{3A,shd}(x,Q^2)$$

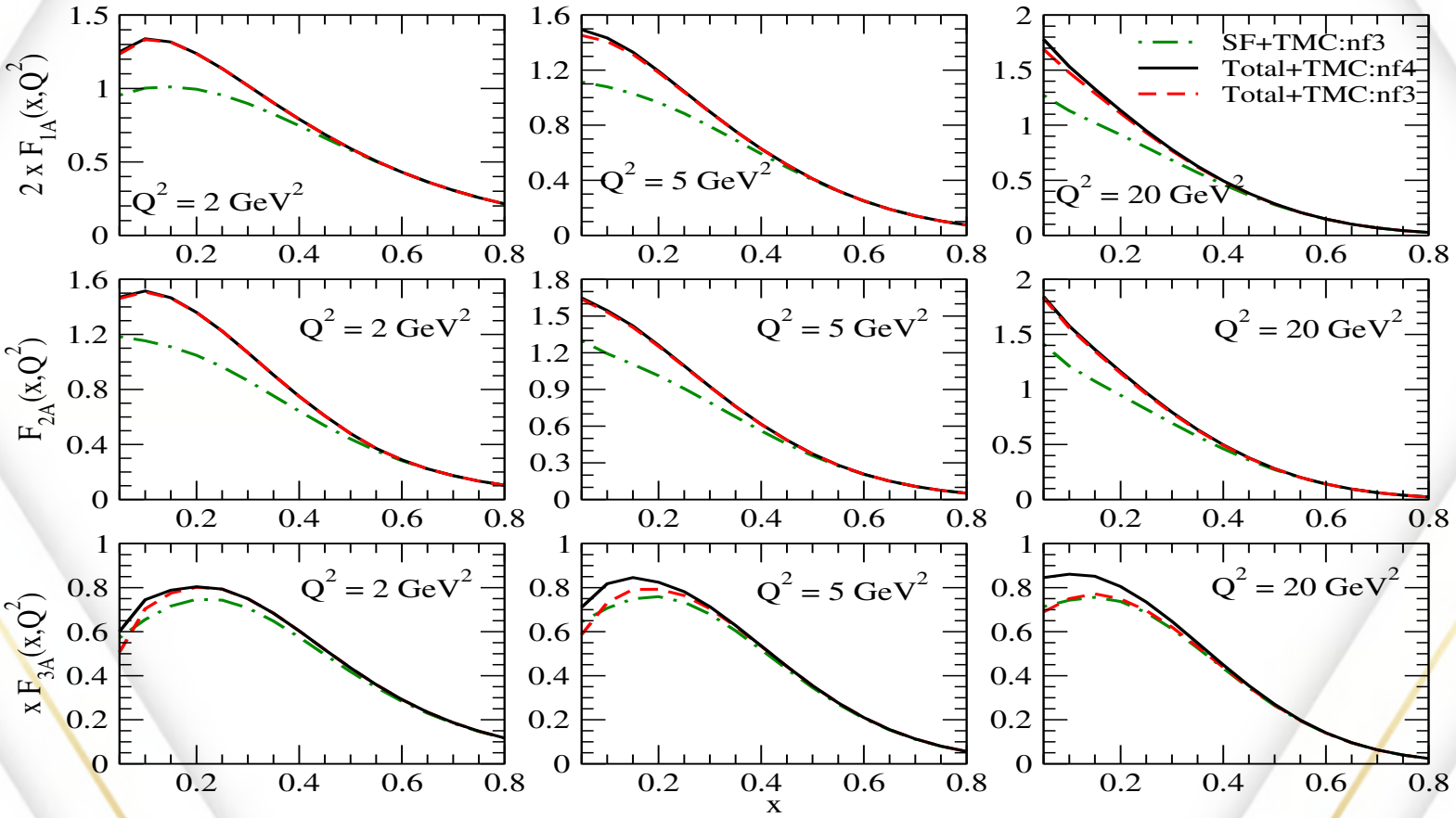

Phys. Rev. D.105 (2022) 3, 033010

Nuclear structure functions: F_{1A}, F_{2A} and F_{3A} vs x in ^{40}Ar

In the full theoretical model:

$$F_{iA}(x,Q^2) = F_{iA,N}(x,Q^2) + F_{iA,\pi}(x,Q^2) + F_{iA,\rho}(x,Q^2) + F_{iA,shd}(x,Q^2);\ \ i = 1-2$$

$$F_{3A}(x,Q^2) = F_{3A,N}(x,Q^2) + F_{3A,shd}(x,Q^2)$$

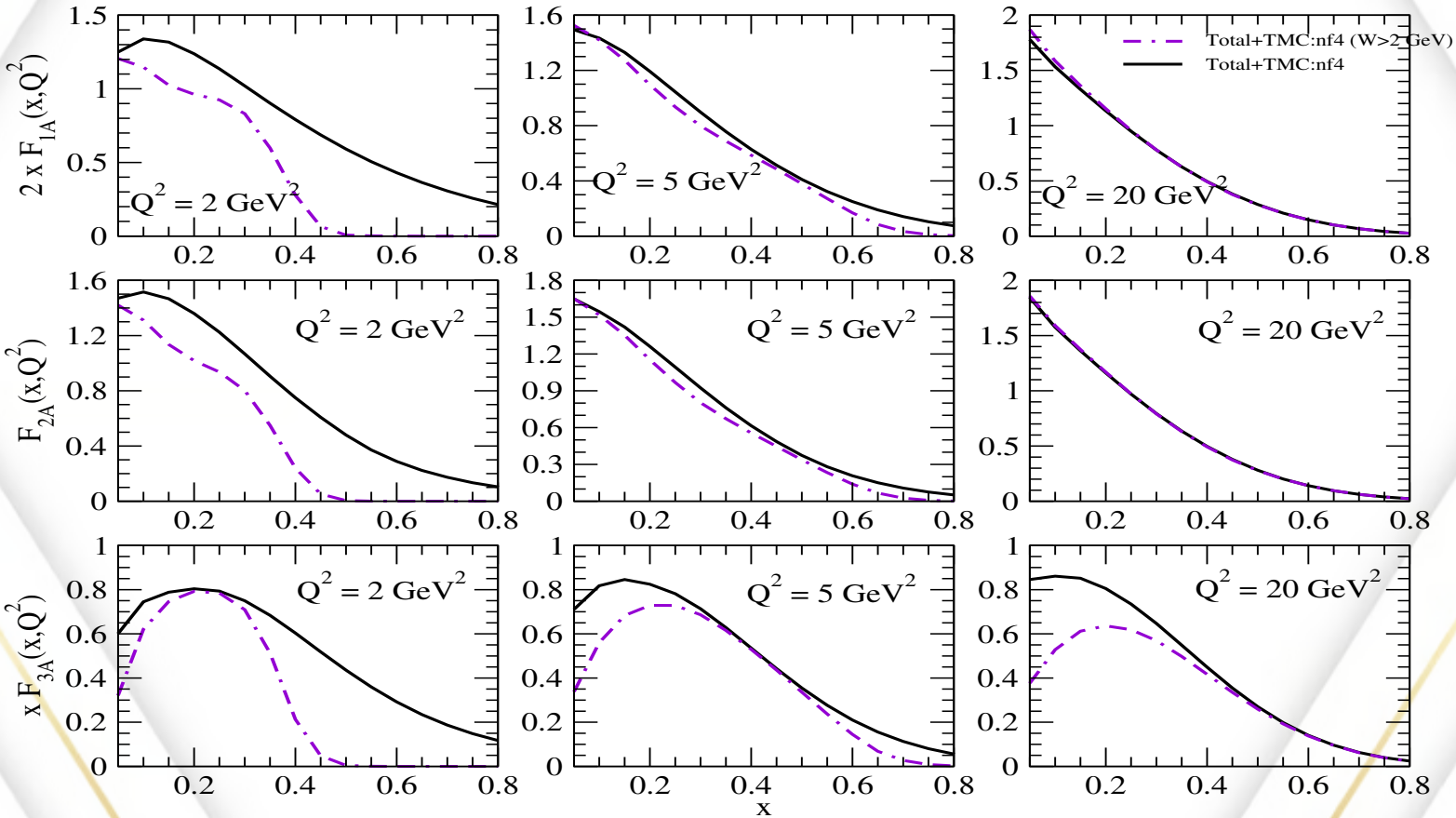

Phys. Rev. D.105 (2022) 3, 033010

Nuclear structure functions: F_{1A}, F_{2A} and F_{3A} vs x in ^{40}Ar

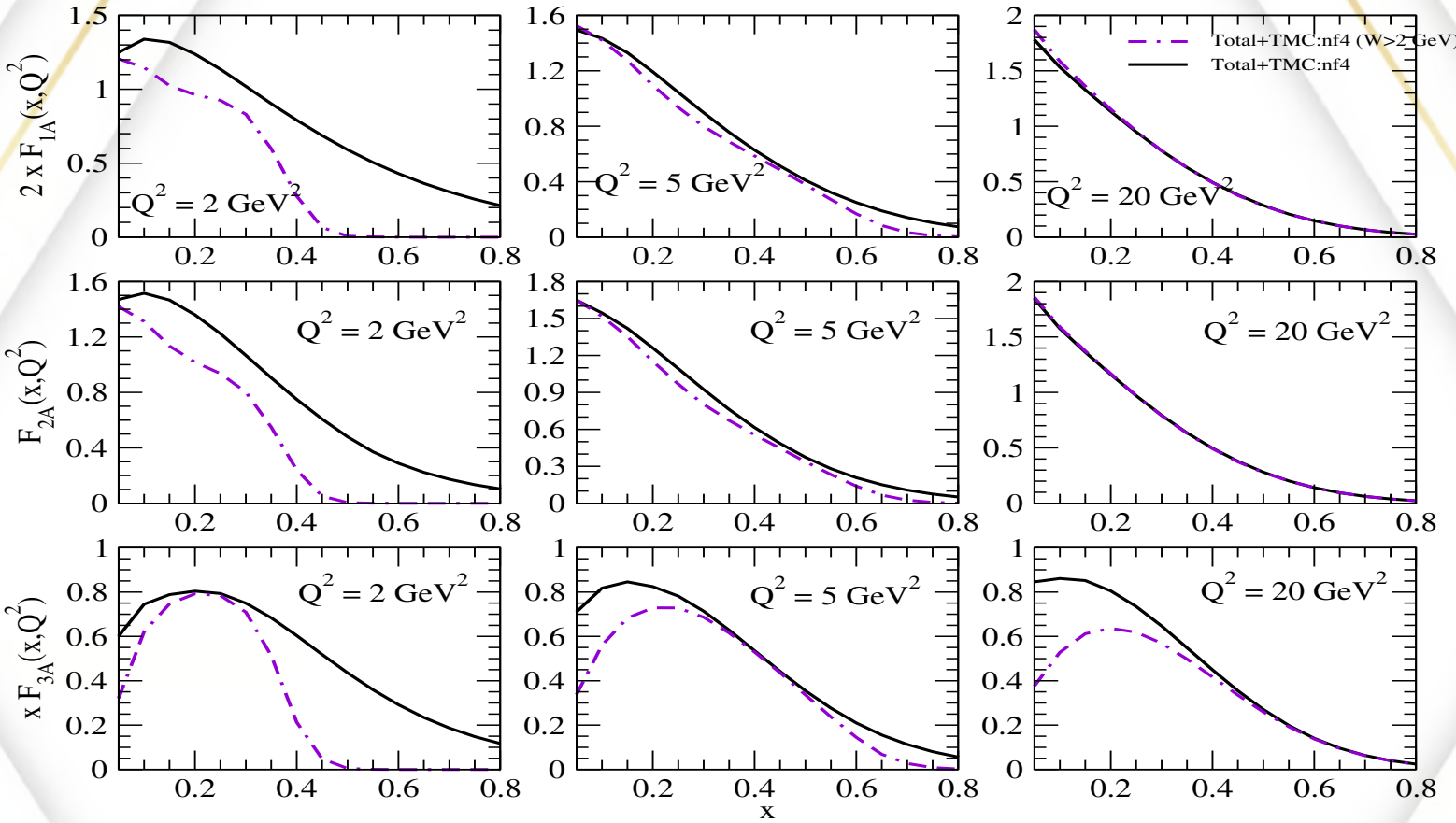

$Q^2(GeV^2)$	x	$(Total^{Nocut} - Total^{Wcut}) * 100/Total^{Nocut}$		
		$F_{1A}(x,Q^2)$	$F_{2A}(x,Q^2)$	$F_{3A}(x,Q^2)$
2	0.1	14%	13%	16%
	0.25	18%	24%	1%
	0.5	≈98%	98%	99%

Nuclear structure functions: F_{4A} and F_{5A} vs x in ^{40}Ar

$$F_{4A}(x,Q^2) = F_{4A,N}(x,Q^2)$$
$$F_{5A}(x,Q^2) = F_{5A,N}(x,Q^2) + F_{5A,\pi}(x,Q^2) + F_{5A,\rho}(x,Q^2) + F_{5A,shd}(x,Q^2)$$

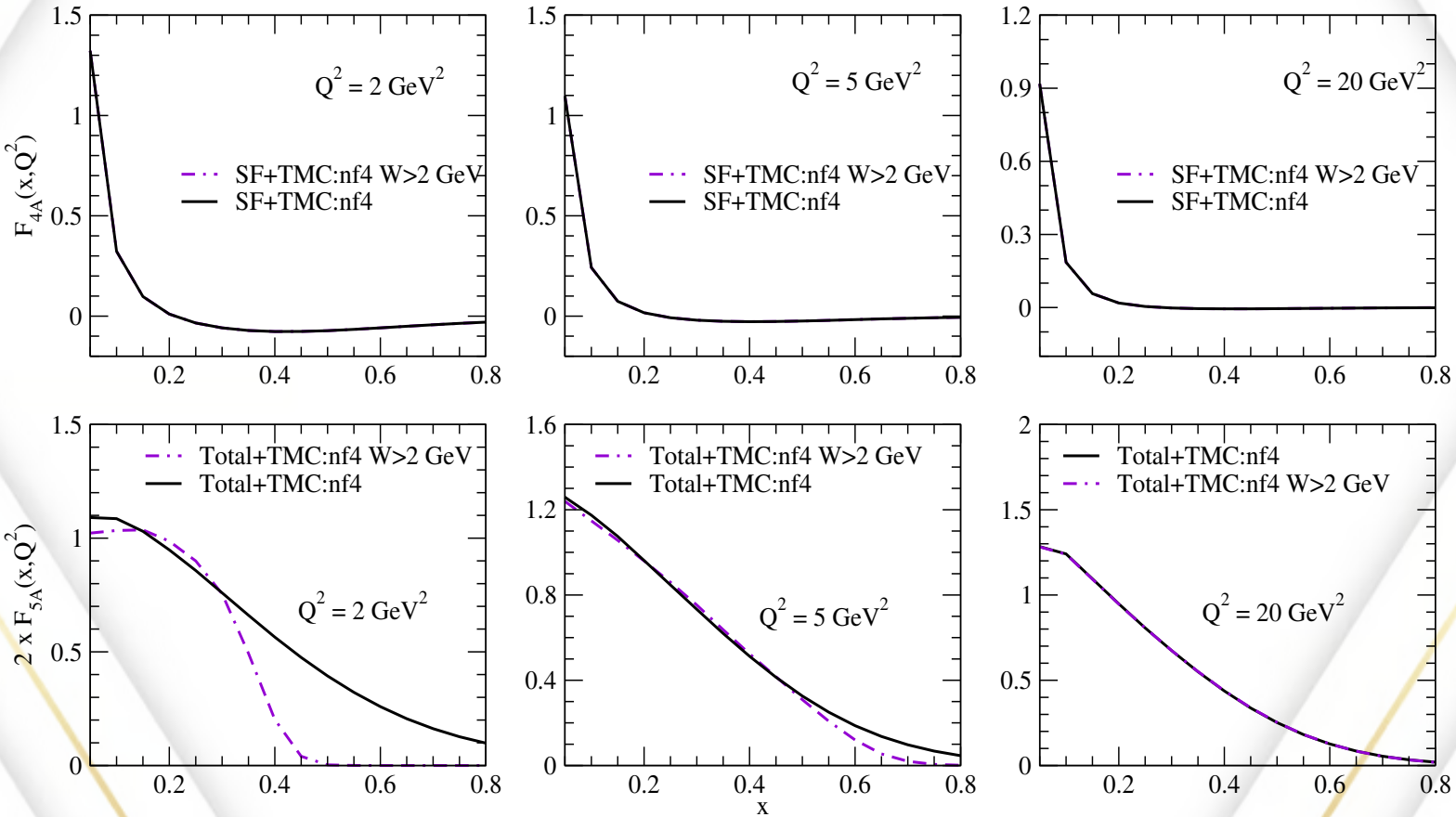

Phys. Rev. D.105 (2022) 3, 033010

Summary

- We observed that the perturbative and nonperturbative effects considered in this work are effective in the various regions of x and Q^2 and quite important in the energy region of $E_{\nu_\tau/\bar{\nu}_\tau} < 15$ GeV.

Summary

- We observed that the perturbative and nonperturbative effects considered in this work are effective in the various regions of x and Q^2 and quite important in the energy region of $E_{\nu_\tau/\bar{\nu}_\tau} < 15$ GeV.
- Massive charm effect is important for the $\nu_\tau - N$ DIS at low x and high Q^2. However, it gets suppressed in the nuclear medium.

Summary

- We observed that the perturbative and nonperturbative effects considered in this work are effective in the various regions of x and Q^2 and quite important in the energy region of $E_{\nu_\tau/\bar{\nu}_\tau} < 15$ GeV.
- Massive charm effect is important for the $\nu_\tau - N$ DIS at low x and high Q^2. However, it gets suppressed in the nuclear medium.
- The effect of $\tau-$lepton mass is found to be significant at low energies in the region of low and intermediate x. However, with the increase in energy the lepton mass effect gradually decreases.

Summary

- We observed that the perturbative and nonperturbative effects considered in this work are effective in the various regions of x and Q^2 and quite important in the energy region of $E_{\nu_\tau/\bar{\nu}_\tau} < 15$ GeV.
- Massive charm effect is important for the $\nu_\tau - N$ DIS at low x and high Q^2. However, it gets suppressed in the nuclear medium.
- The effect of $\tau-$lepton mass is found to be significant at low energies in the region of low and intermediate x. However, with the increase in energy the lepton mass effect gradually decreases.
- The results for the differential scattering cross section with the inclusion of $F_{4N}(x,Q^2)$ and $F_{5N}(x,Q^2)$ structure functions leads to a large reduction in the cross section for ν_τ and $\bar{\nu}_\tau$ scattering on the nucleons especially in the peak region.

Summary

- We observed that the perturbative and nonperturbative effects considered in this work are effective in the various regions of x and Q^2 and quite important in the energy region of $E_{\nu_\tau/\bar{\nu}_\tau} < 15$ GeV.
- Massive charm effect is important for the $\nu_\tau - N$ DIS at low x and high Q^2. However, it gets suppressed in the nuclear medium.
- The effect of $\tau-$lepton mass is found to be significant at low energies in the region of low and intermediate x. However, with the increase in energy the lepton mass effect gradually decreases.
- The results for the differential scattering cross section with the inclusion of $F_{4N}(x,Q^2)$ and $F_{5N}(x,Q^2)$ structure functions leads to a large reduction in the cross section for ν_τ and $\bar{\nu}_\tau$ scattering on the nucleons especially in the peak region.
- Effect of CoM energy cut is significant in the kinematic region of high x, low y and low Q^2 and low energy E. While it decreases with the increase in energy E and Q^2.

Summary

- We observed that the perturbative and nonperturbative effects considered in this work are effective in the various regions of x and Q^2 and quite important in the energy region of $E_{\nu_\tau/\bar{\nu}_\tau} < 15$ GeV.
- Massive charm effect is important for the $\nu_\tau - N$ DIS at low x and high Q^2. However, it gets suppressed in the nuclear medium.
- The effect of $\tau-$lepton mass is found to be significant at low energies in the region of low and intermediate x. However, with the increase in energy the lepton mass effect gradually decreases.
- The results for the differential scattering cross section with the inclusion of $F_{4N}(x,Q^2)$ and $F_{5N}(x,Q^2)$ structure functions leads to a large reduction in the cross section for ν_τ and $\bar{\nu}_\tau$ scattering on the nucleons especially in the peak region.
- Effect of CoM energy cut is significant in the kinematic region of high x, low y and low Q^2 and low energy E. While it decreases with the increase in energy E and Q^2.
- For antineutrino induced process the scattering cross section gets reduced as compared to the case of neutrino induced process which was expected. However, the qualitative behavior of lepton mass effect, center of mass energy cut, massive charm quark and nuclear medium effects are found to be similar.

Summary

- We observed that the perturbative and nonperturbative effects considered in this work are effective in the various regions of x and Q^2 and quite important in the energy region of $E_{\nu_\tau/\bar{\nu}_\tau} < 15$ GeV.
- Massive charm effect is important for the $\nu_\tau - N$ DIS at low x and high Q^2. However, it gets suppressed in the nuclear medium.
- The effect of $\tau-$lepton mass is found to be significant at low energies in the region of low and intermediate x. However, with the increase in energy the lepton mass effect gradually decreases.
- The results for the differential scattering cross section with the inclusion of $F_{4N}(x,Q^2)$ and $F_{5N}(x,Q^2)$ structure functions leads to a large reduction in the cross section for ν_τ and $\bar{\nu}_\tau$ scattering on the nucleons especially in the peak region.
- Effect of CoM energy cut is significant in the kinematic region of high x, low y and low Q^2 and low energy E. While it decreases with the increase in energy E and Q^2.
- For antineutrino induced process the scattering cross section gets reduced as compared to the case of neutrino induced process which was expected. However, the qualitative behavior of lepton mass effect, center of mass energy cut, massive charm quark and nuclear medium effects are found to be similar.
- These theoretical results would be helpful to understand the experimental results from accelerator and atmospheric neutrinos.

“Thank You”

BACK-UP SLIDES

EM nuclear structure functions

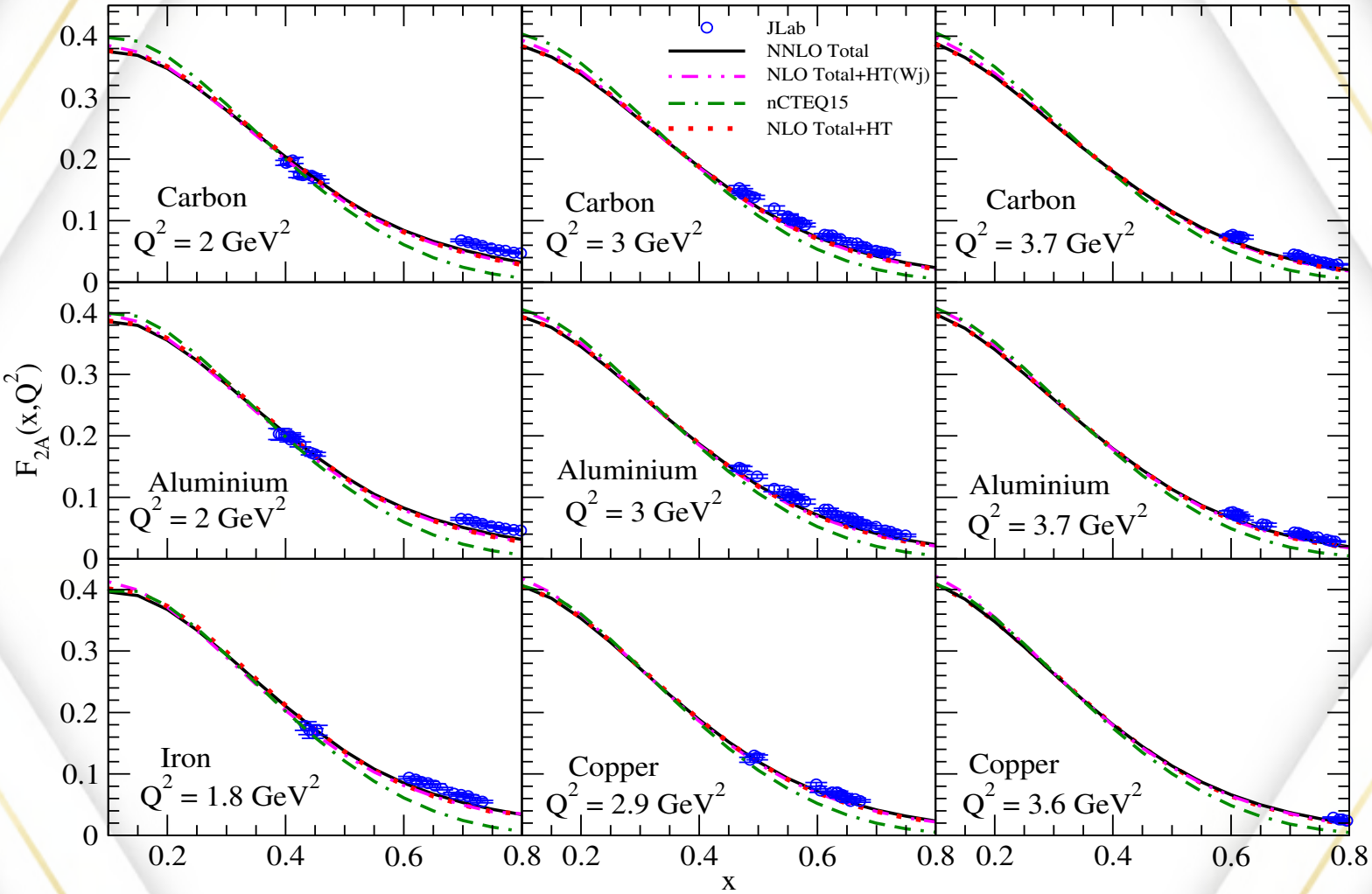

Phys. Rev. D.99 (2019) 3, 093011

EM nuclear structure functions

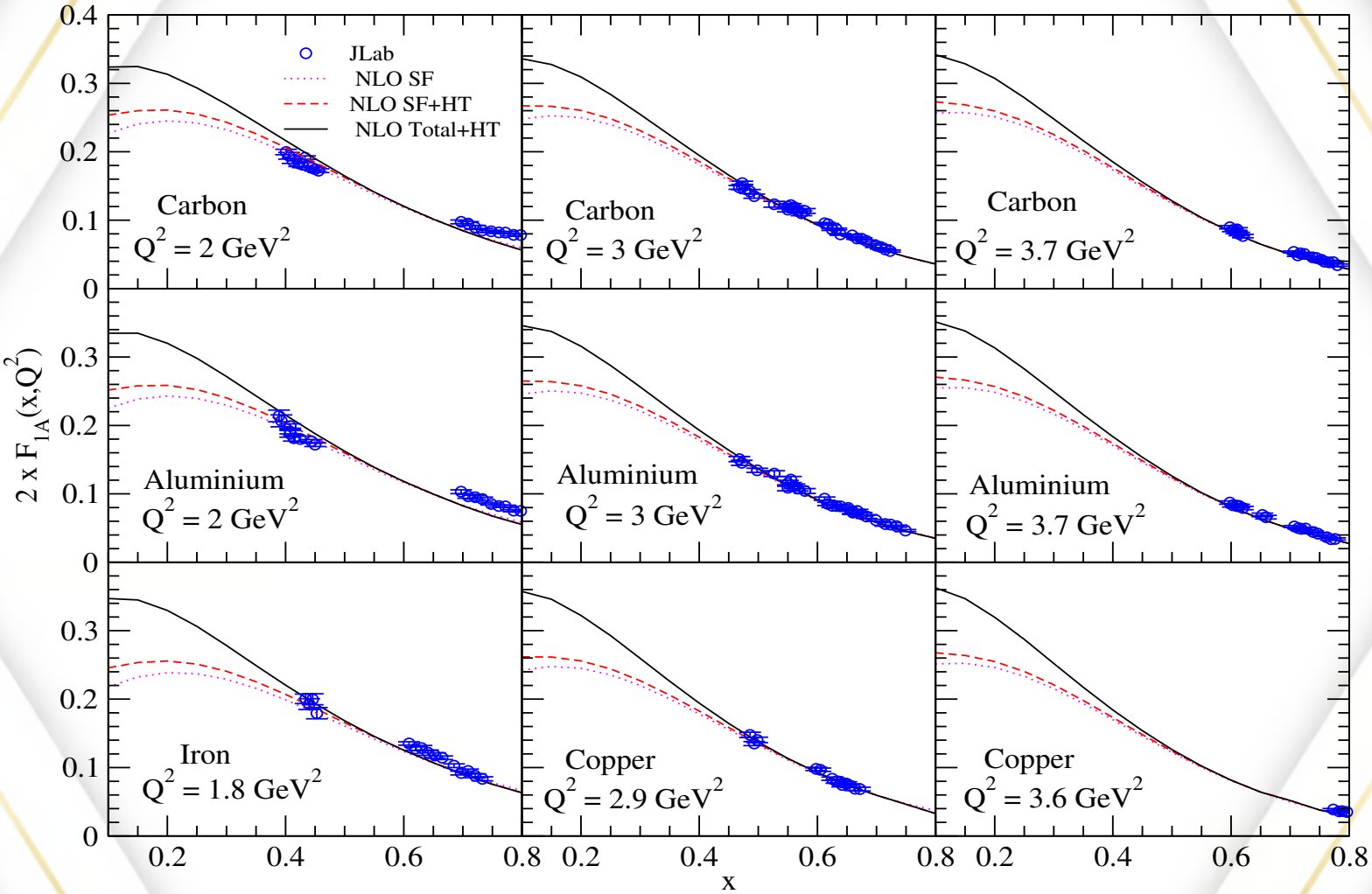

Phys. Rev. D.99 (2019) 3, 093011

EM vs weak nuclear structure functions

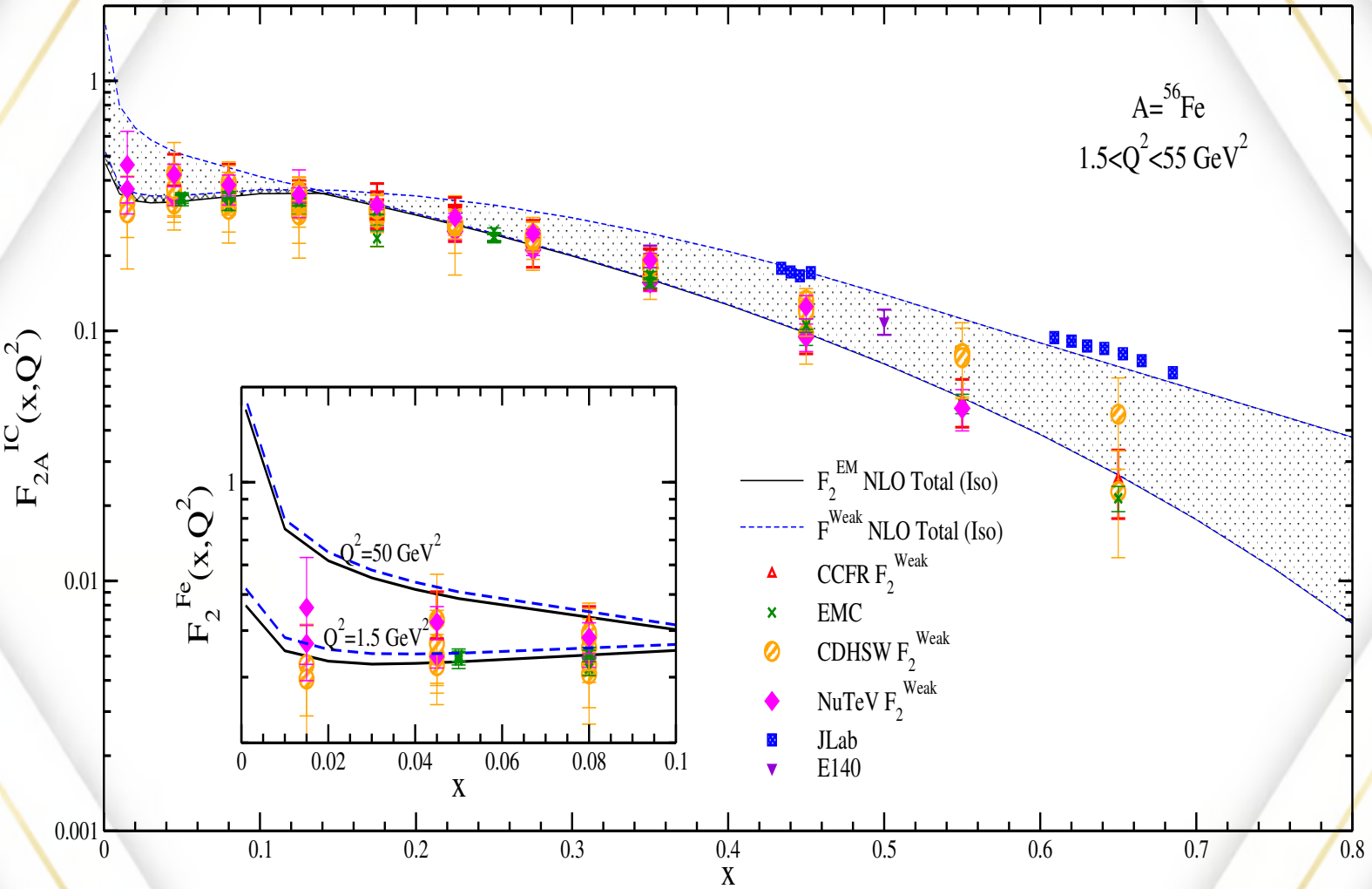

Nucl. Phys. A 955 (2016), 58-78

In the full theoretical model:

$$F_{iA}(x,Q^2) = F_{iA,N}(x,Q^2) + F_{iA,\pi}(x,Q^2) + F_{iA,\rho}(x,Q^2) + F_{iA,shd}(x,Q^2)$$

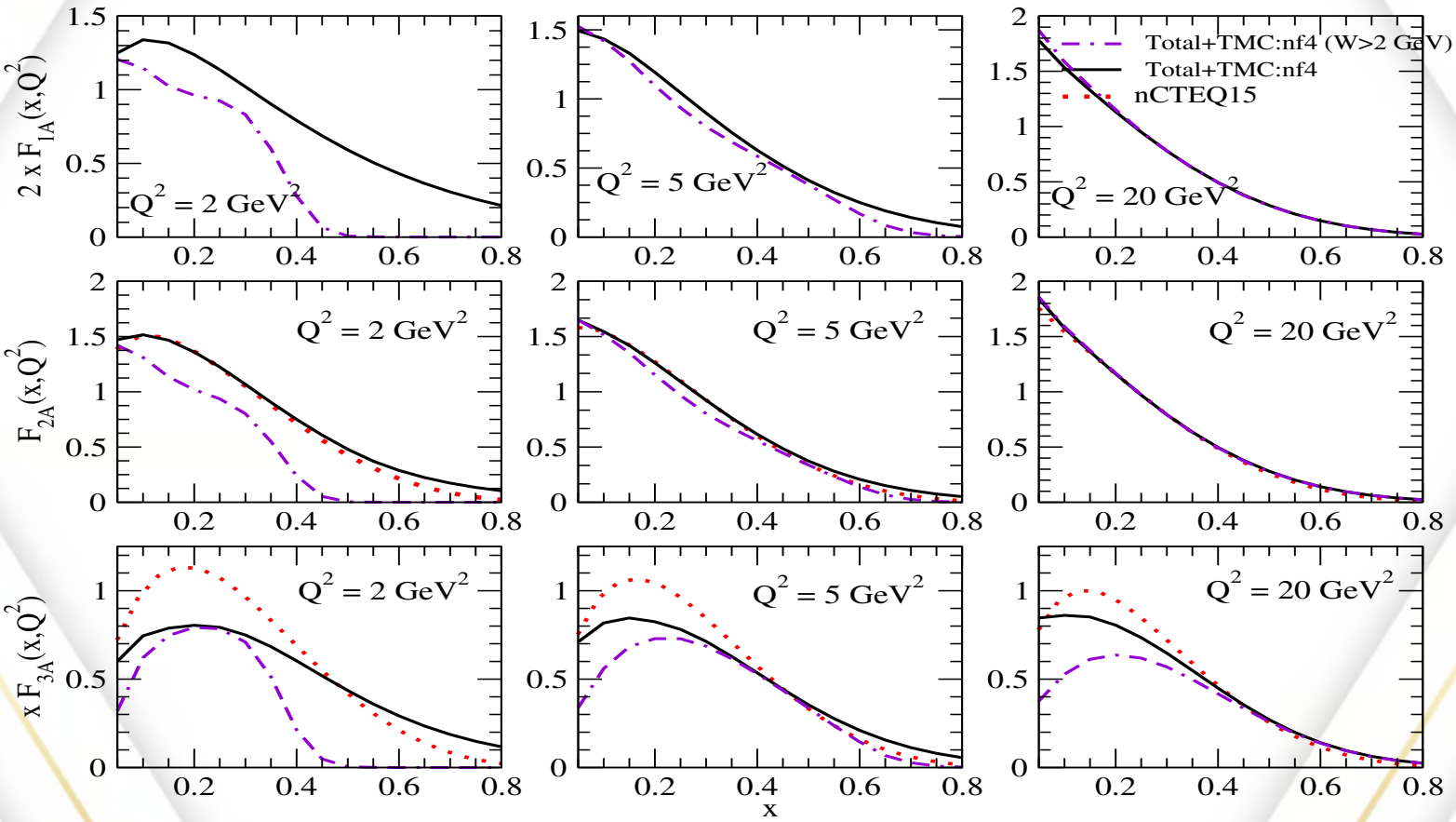

$\frac{1}{E}\frac{d^2\sigma_A}{dxdy}$ vs y at E=10 GeV in ^{40}Ar

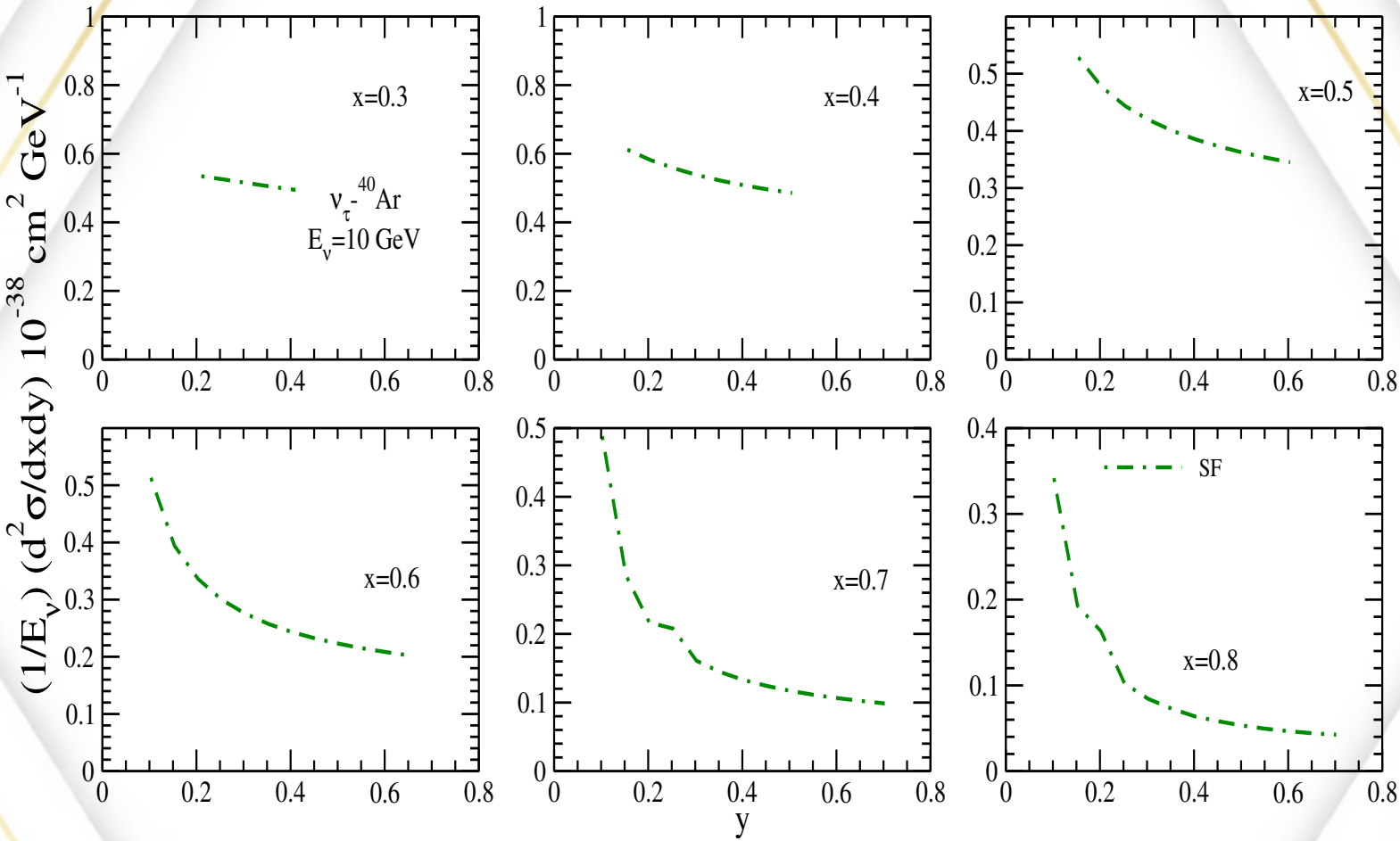

Figure: Results for double differential scattering cross section $\frac{1}{E}\frac{d^2\sigma_A}{dxdy}$ vs y are shown at different x for $E = 10$ GeV in $\nu_\tau - ^{40}Ar$. These results are obtained by incorporating TMC and HT effect at NLO and for the numerical calculations MMHT nucleon PDFs parameterization has been used. These results are also compared with the case when we applied a cut of $W > 1.6$ GeV and $W > 2$ GeV.

Phys. Rev. D.105 (2022) 3, 033010

$\frac{1}{E}\frac{d^2\sigma_A}{dxdy}$ vs y at E=10 GeV in ^{40}Ar

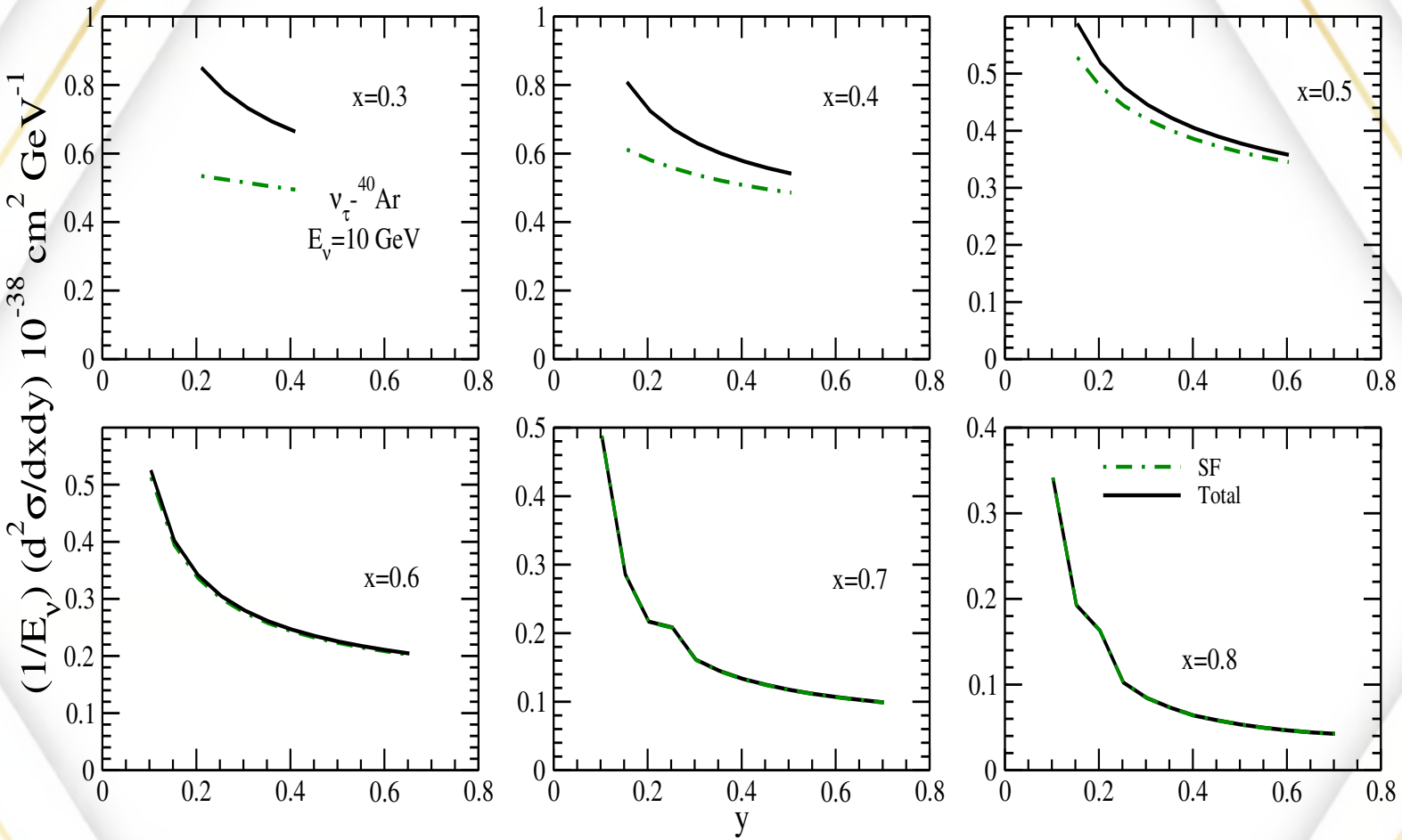

Figure: Results for double differential scattering cross section $\frac{1}{E}\frac{d^2\sigma_A}{dxdy}$ vs y are shown at different x for $E = 10$ GeV in $\nu_\tau - ^{40}Ar$. These results are obtained by incorporating TMC and HT effect at NLO and for the numerical calculations MMHT nucleon PDFs parameterization has been used. These results are also compared with the case when we applied a cut of $W > 1.6$ GeV and $W > 2$ GeV.

Phys. Rev. D.105 (2022) 3, 033010

$\frac{1}{E}\frac{d^2\sigma_A}{dxdy}$ vs y at E=10 GeV in ^{40}Ar

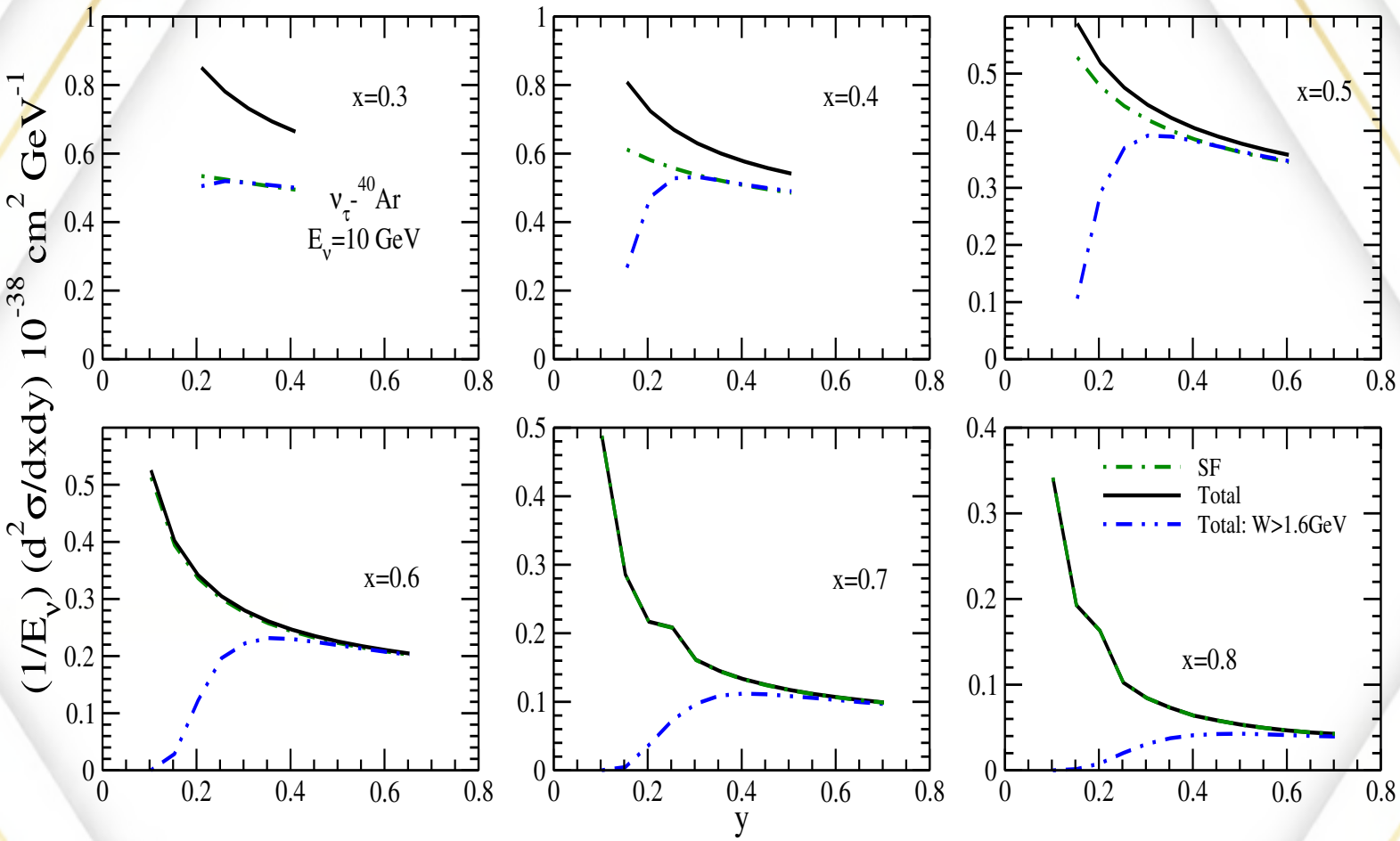

Figure: Results for double differential scattering cross section $\frac{1}{E}\frac{d^2\sigma_A}{dxdy}$ vs y are shown at different x for $E = 10$ GeV in $\nu_\tau - ^{40}Ar$. These results are obtained by incorporating TMC and HT effect at NLO and for the numerical calculations MMHT nucleon PDFs parameterization has been used. These results are also compared with the case when we applied a cut of $W > 1.6$ GeV and $W > 2$ GeV.

Phys. Rev. D.105 (2022) 3, 033010

$\frac{1}{E}\frac{d^2\sigma_A}{dxdy}$ vs y at E=10 GeV in ^{40}Ar

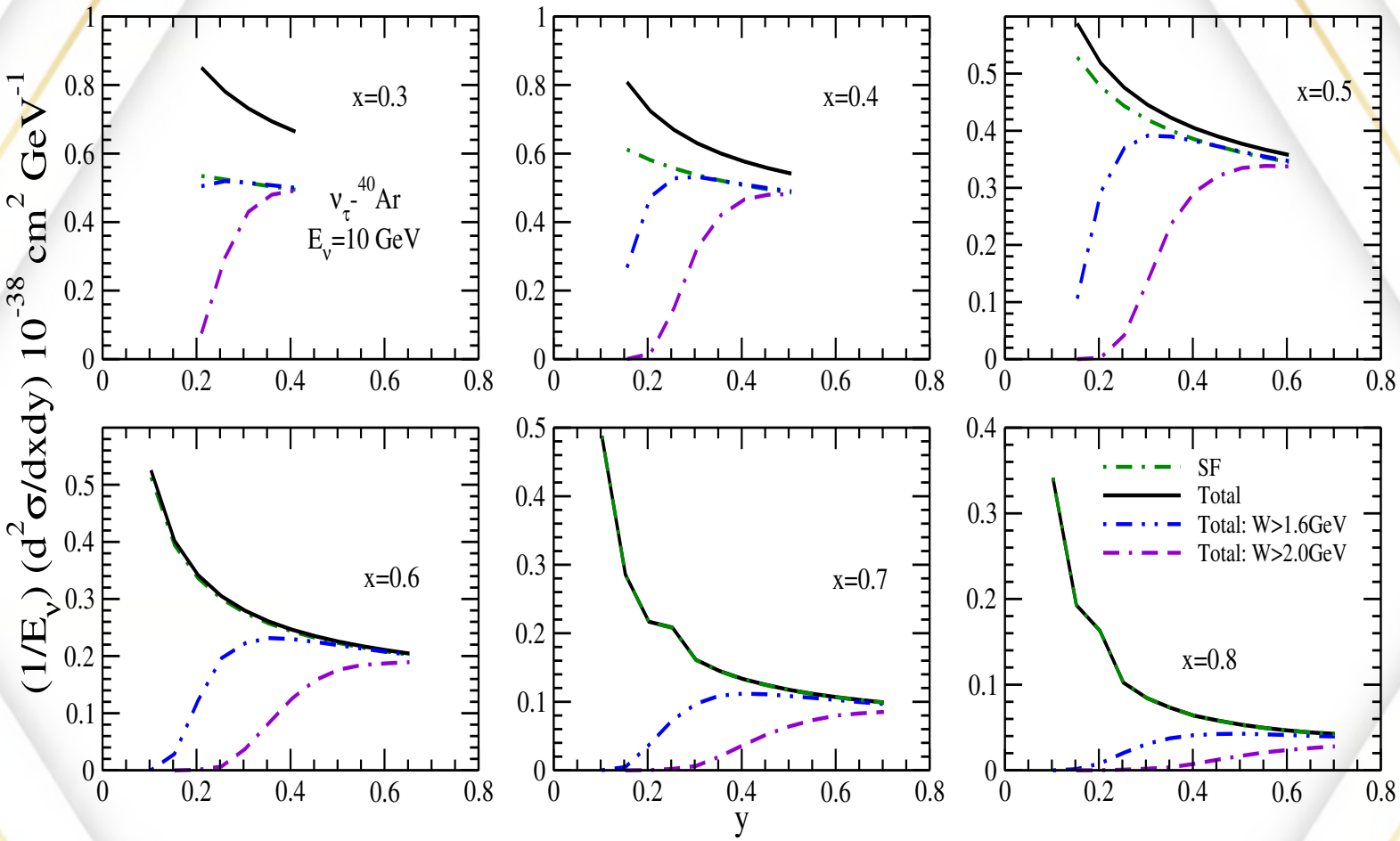

Figure: Results for double differential scattering cross section $\frac{1}{E}\frac{d^2\sigma_A}{dxdy}$ vs y are shown at different x for $E = 10$ GeV in $\nu_\tau - ^{40}Ar$. These results are obtained by incorporating TMC and HT effect at NLO and for the numerical calculations MMHT nucleon PDFs parameterization has been used. These results are also compared with the case when we applied a cut of $W > 1.6$ GeV and $W > 2$ GeV.

Phys. Rev. D.105 (2022) 3, 033010

$\frac{1}{E}\frac{d^2\sigma_A}{dxdy}$ vs y at E=10 GeV in $\bar{\nu}_\tau - {}^{40}Ar$

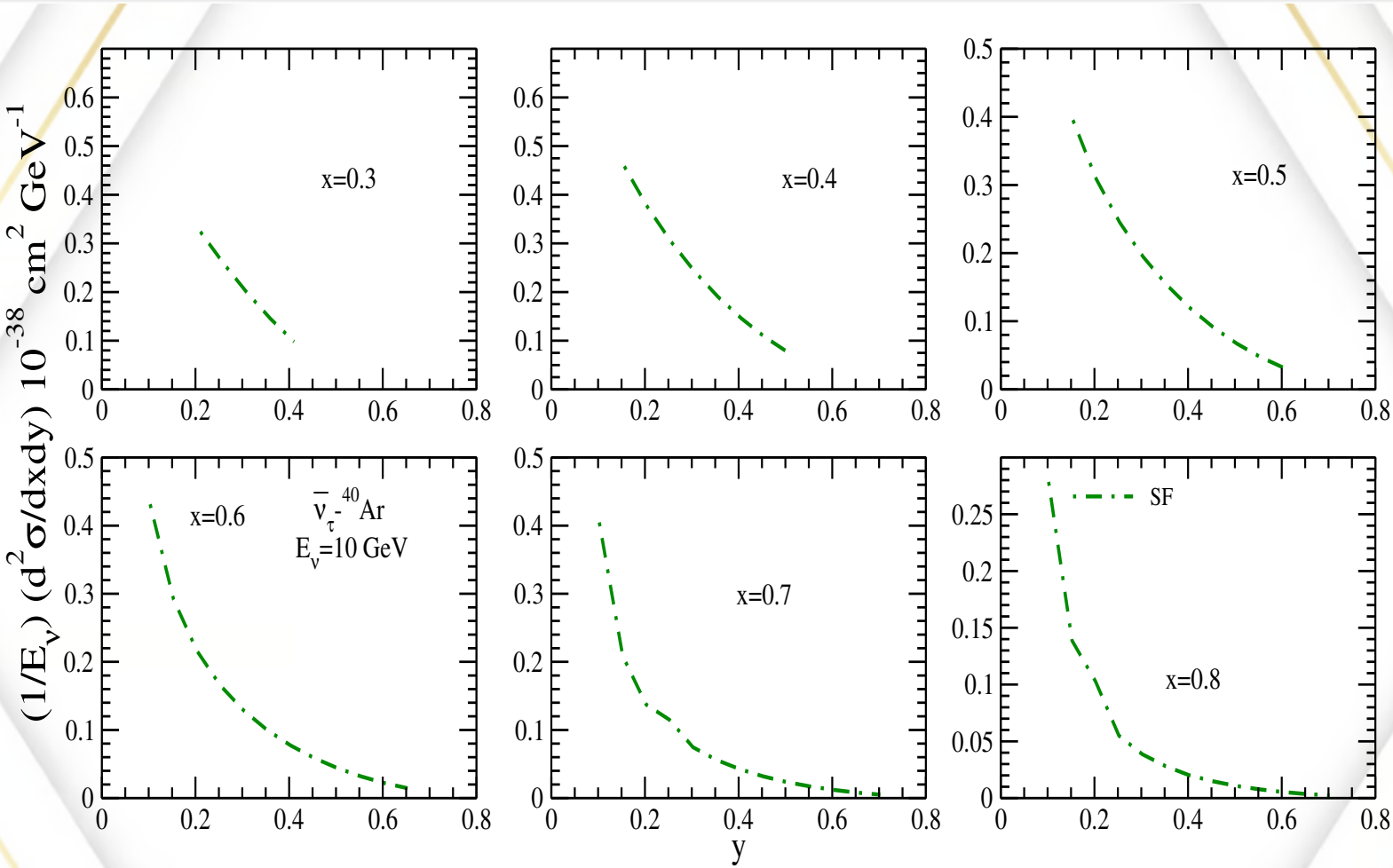

Figure: $\frac{1}{E}\frac{d^2\sigma_A}{dxdy}$ vs y is shown at different x for $E = 10$ GeV in $\bar{\nu}_\tau - {}^{40}Ar$. These results are obtained by incorporating TMC and HT effect at NLO and for the numerical calculations MMHT nucleon PDFs parameterization has been used. These results are also compared with the case when we applied a cut of $W > 1.6$ GeV and $W > 2$ GeV.

Phys. Rev. D.105 (2022) 3, 033010

$\frac{1}{E}\frac{d^2\sigma_A}{dxdy}$ vs y at E=10 GeV in $\bar{\nu}_\tau - {}^{40}Ar$

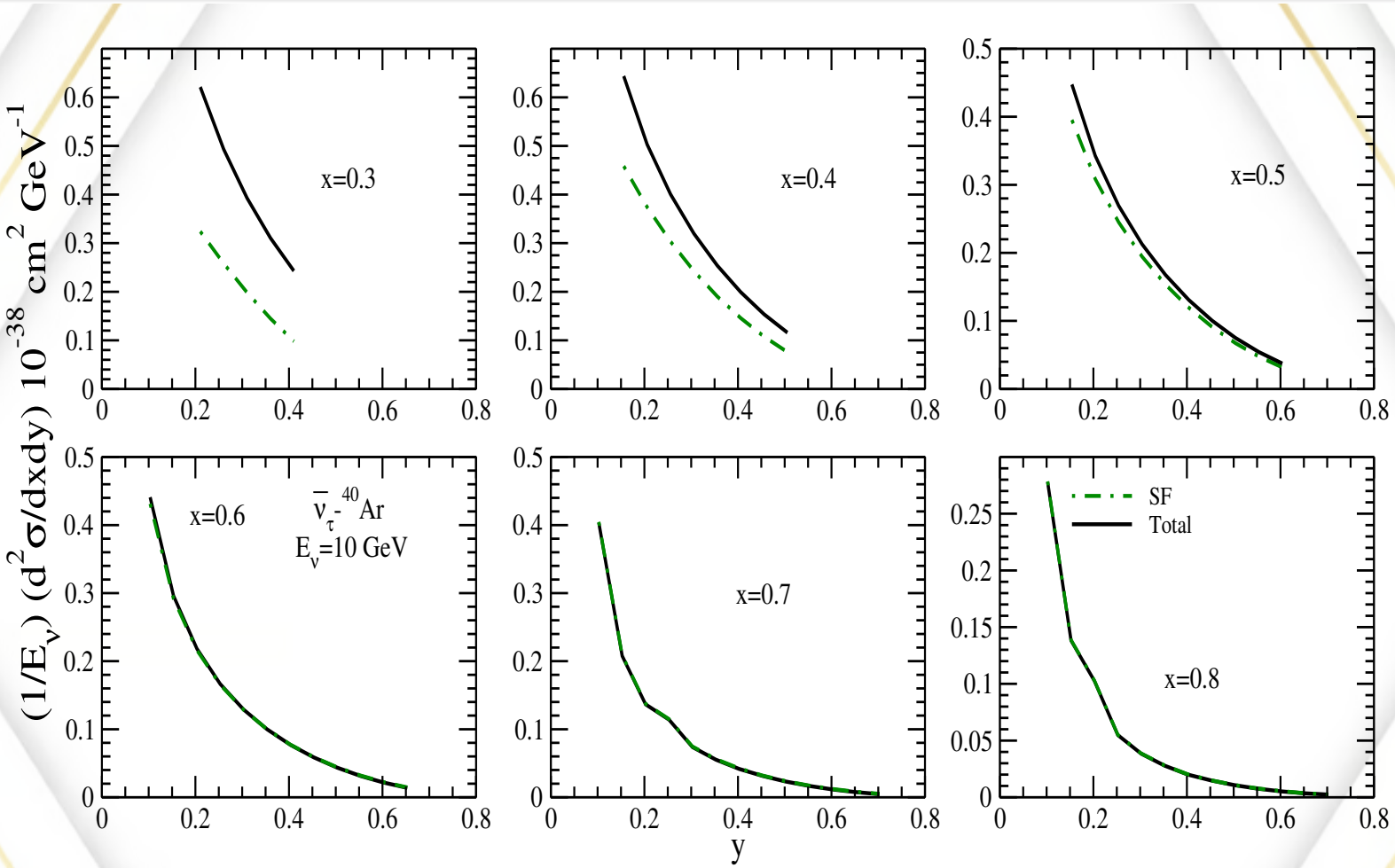

Figure: $\frac{1}{E}\frac{d^2\sigma_A}{dxdy}$ vs y is shown at different x for $E = 10$ GeV in $\bar{\nu}_\tau - {}^{40}Ar$. These results are obtained by incorporating TMC and HT effect at NLO and for the numerical calculations MMHT nucleon PDFs parameterization has been used. These results are also compared with the case when we applied a cut of $W > 1.6$ GeV and $W > 2$ GeV.

Phys. Rev. D.105 (2022) 3, 033010

$\frac{1}{E}\frac{d^2\sigma_A}{dxdy}$ vs y at E=10 GeV in $\bar{\nu}_\tau - {}^{40}Ar$

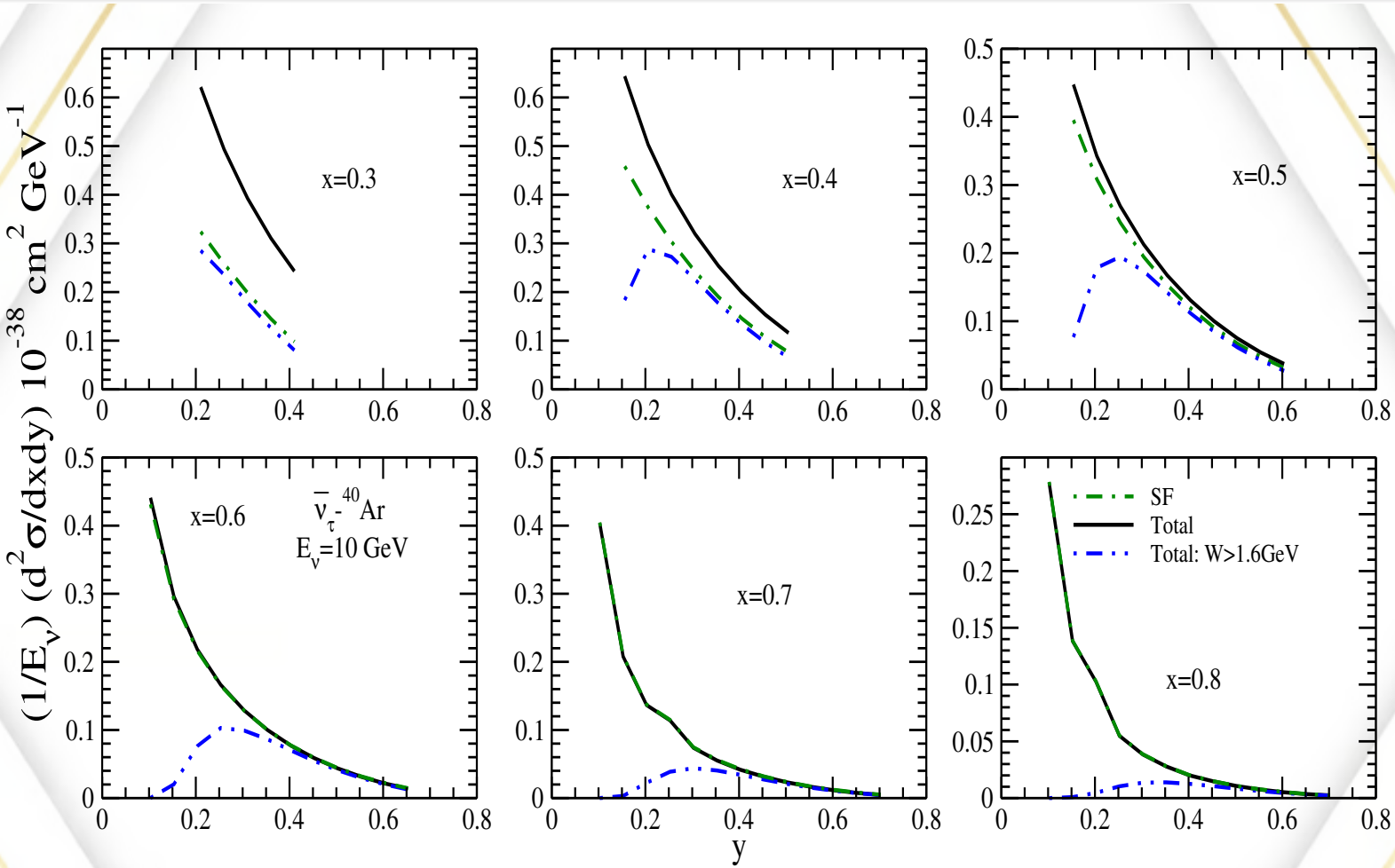

Figure: $\frac{1}{E}\frac{d^2\sigma_A}{dxdy}$ vs y is shown at different x for $E = 10$ GeV in $\bar{\nu}_\tau - {}^{40}Ar$. These results are obtained by incorporating TMC and HT effect at NLO and for the numerical calculations MMHT nucleon PDFs parameterization has been used. These results are also compared with the case when we applied a cut of $W > 1.6$ GeV and $W > 2$ GeV.

Phys. Rev. D.105 (2022) 3, 033010

$\frac{1}{E}\frac{d^2\sigma_A}{dxdy}$ vs y at E=10 GeV in $\bar{\nu}_\tau - {}^{40}Ar$

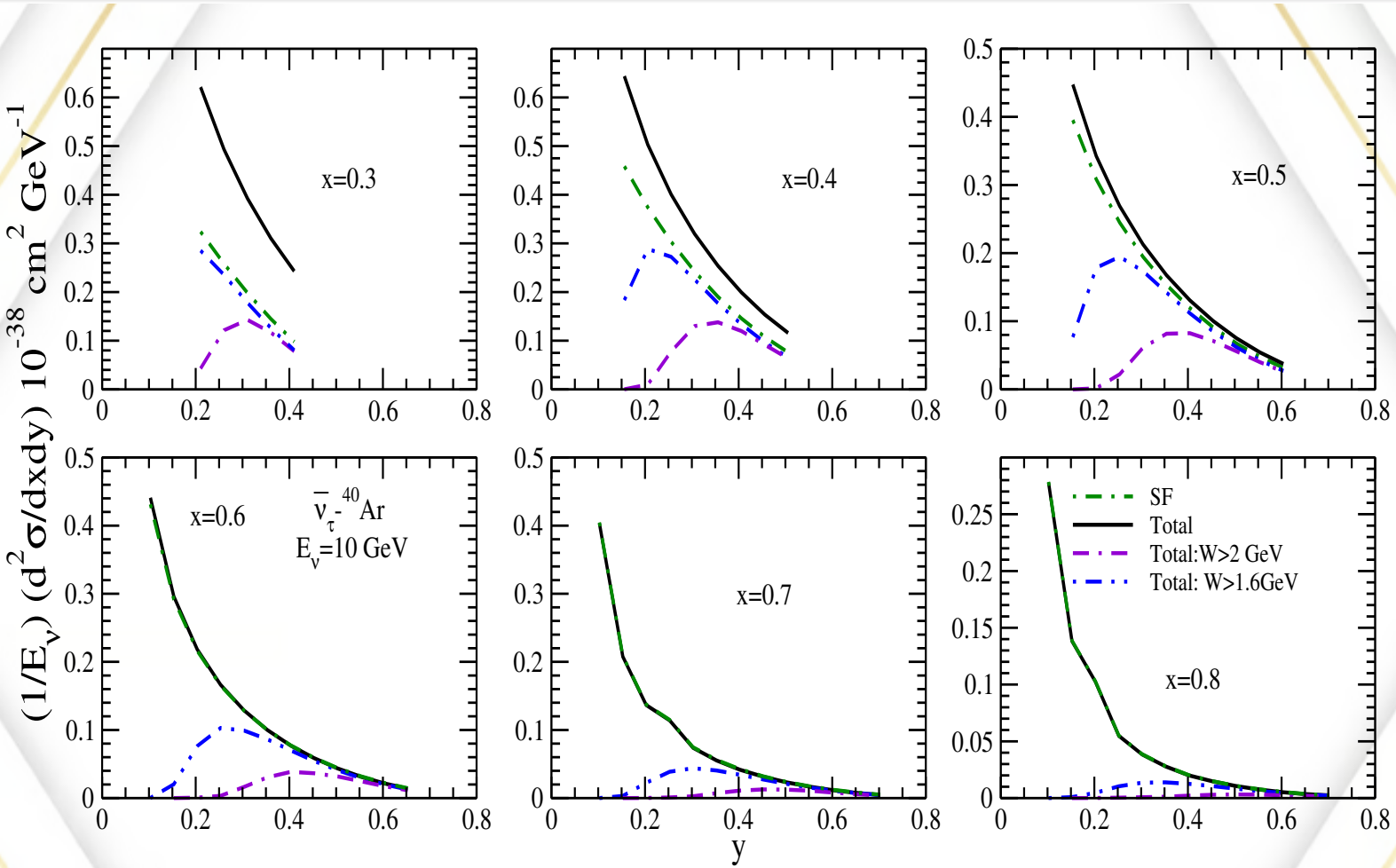

Figure: $\frac{1}{E}\frac{d^2\sigma_A}{dxdy}$ vs y is shown at different x for $E = 10$ GeV in $\bar{\nu}_\tau - {}^{40}Ar$. These results are obtained by incorporating TMC and HT effect at NLO and for the numerical calculations MMHT nucleon PDFs parameterization has been used. These results are also compared with the case when we applied a cut of $W > 1.6$ GeV and $W > 2$ GeV.

Phys. Rev. D.105 (2022) 3, 033010